Voltage- and temperature-dependent activation of TRPV3 channels is potentiated by receptor-mediated PI(4,5)P_2 hydrolysis

Julia F. Doerner,[1] Hanns Hatt,[1] and I. Scott Ramsey[2]

[1]Department of Cell Physiology, Ruhr University Bochum, 44801 Bochum, Germany
[2]Department of Physiology and Biophysics, Virginia Commonwealth University School of Medicine, Richmond, VA 23298

TRPV3 is a thermosensitive channel that is robustly expressed in skin keratinocytes and activated by innocuous thermal heating, membrane depolarization, and chemical agonists such as 2-aminoethyoxy diphenylborinate, carvacrol, and camphor. TRPV3 modulates sensory thermotransduction, hair growth, and susceptibility to dermatitis in rodents, but the molecular mechanisms responsible for controlling TRPV3 channel activity in keratinocytes remain elusive. We show here that receptor-mediated breakdown of the membrane lipid phosphatidylinositol (4,5) bisphosphate (PI(4,5)P_2) regulates the activity of both native TRPV3 channels in primary human skin keratinocytes and expressed TRPV3 in a HEK-293–derived cell line stably expressing muscarinic M_1-type acetylcholine receptors. Stimulation of PI(4,5)P_2 hydrolysis or pharmacological inhibition of PI 4 kinase to block PI(4,5)P_2 synthesis potentiates TRPV3 currents by causing a negative shift in the voltage dependence of channel opening, increasing the proportion of voltage-independent current and causing thermal activation to occur at cooler temperatures. The activity of single TRPV3 channels in excised patches is potentiated by PI(4,5)P_2 depletion and selectively decreased by PI(4,5)P_2 compared with related phosphatidylinositol phosphates. Neutralizing mutations of basic residues in the TRP domain abrogate the effect of PI(4,5)P_2 on channel function, suggesting that PI(4,5)P_2 directly interacts with a specific protein motif to reduce TRPV3 channel open probability. PI(4,5)P_2-dependent modulation of TRPV3 activity represents an attractive mechanism for acute regulation of keratinocyte signaling cascades that control cell proliferation and the release of autocrine and paracrine factors.

The Journal of General Physiology

INTRODUCTION

Transient receptor potential (TRP) channels have emerged as cellular sensors for a variety of environmental and endogenous stimuli (Clapham, 2003). Synthetic and naturally occurring organic compounds (capsaicin, menthol, and 2-aminoethyoxy diphenylborinate [2-APB]), membrane lipids such as phosphatidylinositol phosphates (PIPs) and products of lipid metabolism (diacylglycerol [DAG], eicosanoids, and arachidonate), inorganic ions (Ca^{2+}, Mg^{2+}, and H^+), and transmembrane voltage and temperature changes modulate or directly activate a variety of TRP channels (Ramsey et al., 2006). A subset of "polymodal" TRP channels including TRPV1, TRPV3, TRPA1, TRPM4, and TRPM8 respond to multiple distinct activators, suggesting that they are likely to function as important integrators of convergent cellular stimuli. Depending on the cell- and tissue-specific contexts of their expression, polymodal TRP channels are poised to perform a variety of physiological functions in health and disease (Nilius, 2007).

TRPV3 (human TRP channel, vanilloid family, subtype 3; NCBI Protein database accession no. AF514998) is a Ca^{2+}-permeable cation channel that is activated by moderate thermal heating (≥32°C) in the range where warmth is sensed (Peier et al., 2002; Smith et al., 2002; Xu et al., 2002). Organic chemicals such as 2-APB and structurally related compounds, plant-derived compounds (camphor, carvacrol, and thymol), and unsaturated fatty acids also activate or potentiate TRPV3 activation (Peier et al., 2002; Smith et al., 2002; Xu et al., 2002, 2005, 2006; Chung et al., 2004a; Hu et al., 2006; Phelps et al., 2010). TRPV3 also displays an unusual sensitization to repeated activation that was attributed to modulation of channel activity by Ca^{2+} and calmodulin (Xiao et al., 2008a; Phelps et al., 2010). TRPV3 protein and mRNA are highly expressed in epidermal keratinocytes, and TRPV3 currents were reported in primary rodent keratinocytes and immortalized 308 cells (Peier et al., 2002; Smith et al., 2002; Xu et al., 2002, 2006; Chung et al., 2003, 2004b; Hu et al., 2006; Cheng et al., 2010). Targeted deletion of TRPV3 in mice abolishes TRPV3 currents in keratinocytes, causes a

Correspondence to I. Scott Ramsey: isramsey@vcu.edu
J.F. Doerner's present address is Dept. of Cardiology, Children's Hospital Boston, and Dept. of Neurobiology, Harvard Medical School, Boston, MA 02115.

Abbreviations used in this paper: 2-APB, 2-aminoethyoxy diphenylborinate; CCh, carbamylcholine; DAG, diacylglycerol; OAG, 1-oleoyl-2-acetyl-*sn*-glycerol; PAO, phenylarsine oxide; PI(4,5)P_2, phosphatidylinositol (4,5) bisphosphate; PIP, phosphatidylinositol phosphate; PI-PLC, phosphatidylinositol-specific PLC; TRP, transient receptor potential; VIF, voltage-independent fraction; WM, wortmannin; WT, wild type.

The Rockefeller University Press $30.00
J. Gen. Physiol. Vol. 137 No. 3 271–288
www.jgp.org/cgi/doi/10.1085/jgp.200910388

wavy hair/curly whisker phenotype and erythroderma, and alters thermal selection, indicating that the channel is necessary for normal hair development, epidermal barrier formation, and thermosensation (Moqrich et al., 2005; Cheng et al., 2010). In addition, the release of ATP and transforming growth factor α (TGF-α) elicited by TRPV3 agonists and thermal warming of primary keratinocytes is attenuated in TRPV3-null mice (Mandadi et al., 2009; Cheng et al., 2010). Keratinocyte secretion of chemical messengers and growth factors thus transmits important information to proliferating and differentiating keratinocyte as well as sensory neurons (Lee and Caterina, 2005; Lumpkin and Caterina, 2007; Mandadi et al., 2009; Cheng et al., 2010). Interestingly, spontaneous autosomal dominant mutations in TRPV3 that result in constitutive channel activity cause hairlessness and increase susceptibility to dermatitis and inflammatory skin lesions in rodents (Asakawa et al., 2006; Xiao et al., 2008b; Imura et al., 2009; Yoshioka et al., 2009). TRPV3-mediated Ca^{2+} influx and depolarization may therefore represent an important link in signaling cascades that control cellular activation, the release of autocrine and paracrine factors, hair morphogenesis, and cell proliferation in keratinocytes.

Studies performed using heterologous expression systems showed that TRPV3 currents are also strongly potentiated by stimulation of $G_{q/11}$-coupled receptors in a PLCβ-dependent fashion (Xu et al., 2006). Activation of PLC-coupled growth factor receptors also enhances TRPV3-dependent Ca^{2+} influx (Cheng et al., 2010). The precise mechanism of TRPV3 potentiation by PLC-coupled receptors is unknown, but the response is inhibited by U73122, suggesting that stimulation of PLC activity may relieve a tonic inhibitory influence on channel opening that limits the amount of TRPV3 current under resting conditions (Xu et al., 2006; Cheng et al., 2010). PLCβ mediates hydrolysis of plasma membrane phosphatidylinositol (4,5) bisphosphate ($PI(4,5)P_2$), which is known to modulate the activity of a plethora of ion channels and transporters in the plasma membrane, including several members of the TRP channel family (Gamper and Shapiro, 2007; Rosenhouse-Dantsker and Logothetis, 2007; Nilius et al., 2008; Suh and Hille 2008; Rohács, 2009). We therefore hypothesized that TRPV3 channel activity might be negatively regulated by resting levels of $PI(4,5)P_2$, such that $G_{q/11}$-coupled receptor activation would result in an increase in TRPV3 conductance.

Elucidating the mechanisms by which PIPs regulate the function of ion channels and transporters is an area of active investigation, but the details of protein–PIP interactions are not well understood. Putative $PI(4,5)P_2$-binding motifs identified in various integral membrane proteins commonly contain several basic amino acid residues that are predicted to form electrostatic interactions with negatively charged phosphates on the inositol ring, but lipid contacts with noncharged residues are likely to contribute to PIP specificity; to date, no consensus $PI(4,5)P_2$-binding sequence has emerged (Rosenhouse-Dantsker and Logothetis, 2007; Suh and Hille, 2008). In TRPV1, TRPV5, TRPM5, and TRPM8, modulation of channel activity by $PI(4,5)P_2$ is sensitive to mutations of residues located in the TRP domain, an ∼25-residue motif that is conserved in most TRP channel subfamilies (Nilius et al., 2008; Rohács, 2009). Within the TRP domain is a six–amino acid TRP box motif that typically contains at least two basic residues interspersed with hydrophobic amino acids and is predicted to form an amphipathic helix (Montell, 2001; Ramsey et al., 2006; Brauchi et al., 2007). A nearby poly basic motif, which is found C-terminal to the TRP domain, has also been implicated in $PI(4,5)P_2$ binding to TRPV1 (Ufret-Vincenty et al., 2011). The functional consequences of $PI(4,5)P_2$ binding range from inhibition (Estacion et al., 2001; Otsuguro et al., 2008) to bidirectional modulation (Chuang et al., 2001; Stein et al., 2006; Lukacs et al., 2007) to activation (Runnels et al., 2002; Liu and Liman, 2003; Liu and Qin, 2005; Rohács et al., 2005; Nilius et al., 2006; Karashima et al., 2008; Mercado et al., 2010; Ufret-Vincenty et al., 2011).

We show here that the activation of $G_{q/11}$-coupled receptors alters the voltage dependence of activation and potentiates the amplitude of current carried by endogenous TRPV3 channels in primary human keratinocytes. The activation of M_1 receptors in HM1 cells (HM1 is a HEK-293 cell clone that stably expresses the $G_{q/11}$-coupled human muscarinic acetylcholine receptor type 1 [M_1]) (Peralta et al., 1988) additionally sensitizes recombinant TRPV3 channels to activation by thermal heating and increases the potency of the channel agonist 2-APB. Pharmacological depletion of membrane $PI(4,5)P_2$ mimics the effect of $G_{q/11}$-coupled receptor stimulation. In excised patches, the open probability of TRPV3 single-channel currents is reduced by a water-soluble $PI(4,5)P_2$ analogue. Finally, we identify two basic residues in the TRP domain that are required for $PI(4,5)P_2$-dependent modulation of TRPV3. The majority of our data are well explained by a mechanism that involves tonic suppression of TRPV3 channel activity by $PI(4,5)P_2$ and rapid relief by receptor-mediated activation of PLCβ.

MATERIALS AND METHODS

DNA constructs, cells, and transfection

cDNA encoding human TRPV3 (Xu et al., 2002) was subcloned into pIRES-EGFP (Invitrogen) as an EcoRV/NotI fragment for expression in mammalian cells. TRPV3 R696A and K705A mutagenesis was performed using overlap extension PCR with synthetic complementary oligonucleotides (Ho et al., 1989). All cDNA mutations were verified by DNA sequencing. HM1 cells (Peralta et al., 1988) were maintained in DMEM supplemented with 10% fetal bovine serum, 100 µg/ml penicillin/streptomycin (Invitrogen), and 0.5 mg/ml G-418 (A.G. Scientific, Inc.) at 37°C, 5% CO_2. Cells were transfected using the calcium phosphate precipitation method

(Zufall et al., 1993). Transfected cells were trypsinized and plated onto glass coverslips and used for electrophysiological recordings 24–48 h after transfection. Transfected cells were identified by GFP fluorescence before electrophysiological recording.

Freshly collected human skin was processed as described by Jacobsen et al. (2005). Human keratinocytes were provided by the BG University Hospital Bergmannsheil (Ruhr University, Bochum, Germany) and maintained in complete keratinocyte medium (DMEM/Ham's F12 [3:1; Invitrogen], 10% FBS, 1% penicillin/streptomycin [Invitrogen], 5 µg/ml human insulin [Sigma-Aldrich], 24.3 µg/ml adenine [Sigma-Aldrich], 1 µM isoproterenol [Sigma-Aldrich], 0.8 µg/ml hydrocortisone [Sigma-Aldrich], 1.36 ng/ml triiodothyronine [Sigma-Aldrich], and 20 ng/ml human EGF [Sigma-Aldrich]) at 37°C, 5% CO_2, for four passages. Keratinocytes were trypsinized and plated onto glass coverslips for electrophysiological recordings 24–48 h later.

Electrophysiology

The standard bath solution used for whole cell recordings contained (in mM): 139 NaCl, 5 KCl, 10 HEPES, 10 glucose, 2 $MgCl_2$, and 1.8 $BaCl_2$, pH 7.4 with NaOH. The pipette solution used to acquire 2-APB concentration–response curves and heat-evoked currents contained (in mM): 120 cesium methanesulfonate ($CsMeSO_3$), 10 EGTA, 10 HEPES, 2 $MgCl_2$, and 3.15 $CaCl_2$ (free [Ca^{2+}] ≈ 50 nM), pH 7.3 with CsOH. For experiments involving muscarinic and purinergic receptor activation, the pipette solution contained (in mM): 120 $CsMeSO_3$, 10 1,2-Bis(2-aminophenoxy)ethane-*N,N,N′,N′*-tetraacetic acid (BAPTA), 10 HEPES, 2 $CaCl_2$ (free [Ca^{2+}] ≈ 50 nM), 0.3 Na-GTP, 2 Mg-ATP, and 8 NaCl, pH 7.3 with CsOH. Ca^{2+}-free pipette solution contained (in mM): 120 $CsMeSO_3$, 10 BAPTA, 10 HEPES, 0.3 Na-GTP, 2 Mg-ATP, and 12 NaCl (free [Ca^{2+}] < 10 nM), pH 7.3 with CsOH. The development of nonspecific leak currents during thermal heating was assessed by superfusing an Na^+-free bath solution (in mM: 150 NMDG, 10 HEPES, and 10 glucose, pH 7.4 with HCl) at the peak of the temperature ramp. Cells displaying measurable inward currents in the presence of NMDGCl were omitted from analysis. The pipette and bath solution used for excised inside-out patch recordings was symmetrical (in mM): 145 NaCl, 5 $CsCl_2$, 20 HEPES, and 1 EGTA, pH 7.4 with NaOH. Inside-out patches were washed by bath superfusion after excision and reagents were added by perfusion (~1 min), followed by incubation in a still bath chamber (total time of exposure to the indicated reagents is indicated by horizontal bars in the figures); subsequent washout was accomplished by restarting the superfusion. For cell-attached recordings, NaCl in the bath solution was replaced by KCl. Free calcium concentrations were calculated using MaxChelator.

Unless otherwise indicated, recordings were performed at room temperature (21–24°C). In some experiments, bath solution was regulated using a bipolar temperature controller and an in-line heater/cooler with continuous superfusion (Warner Instruments). The temperature of the superfusate was recorded using a thermistor placed in close proximity to the cell.

Membrane voltage was controlled and currents were recorded using an amplifier (EPC7 Plus; HEKA) interfaced with a PC computer running Pulse and PulseFit software (HEKA). Whole cell current recordings were acquired at 5–10 kHz and low-pass filtered at 2 kHz. Capacitance correction and series resistance compensation (30–50%) were routinely used. Excised patch recordings were acquired at 10 kHz and low-pass filtered at 5 kHz. Currents were further digitally filtered offline for display purposes. For both wild-type (WT) TRPV3 and TRP domain mutants, currents were activated by 2-APB at 0.3 times its respective [EC_{50}] to minimize irreversible entry of channels into the I2 conducting state and to control for changes in 2-APB potency observed in TRPV3 mutants.

Data analysis

Data were analyzed using Pulse and PulseFit (HEKA), OriginPro (OriginLab), IgorPro (WaveMetrics), Clampfit 9 (Axon Instruments), and Excel (Microsoft). Data are expressed as mean ± SEM unless otherwise noted. Statistical comparisons were made using Student's unpaired *t* test. Concentration–response relations were fitted with a Hill equation of the form $I = I_{max}([X]^n/EC_{50}{}^n + [X]^n)$, where I is current, [X] is ligand concentration, EC_{50} is half-maximal current, and n is the Hill coefficient. In some cases, n was constrained during the curve fitting. The thermal coefficient (Q_{10}) for temperature-dependent activation of TRPV3 currents was calculated from the slope of the steep phase of log(*I*) versus 1,000/T (1/°K) plots, determined by linear regression fits (y = A + B * X, where B is the slope and A is the intercept). Peak tail current amplitude (I_{TAIL}) was calculated by extrapolating the time-decaying current to the instant of membrane voltage change (t = 0) using mono-exponential fits. The I_{TAIL}–V relation for each cell was fitted to a Boltzmann function ($I = I2 + (I1–I2)/(1 + \exp((V–V_0)/dV))$, where I is current, I1 is current minimum, I2 is current maximum, and V is membrane voltage). Where the data were not well fit to a complete Boltzmann function (i.e., in the absence of 2-APB), we empirically determined an apparent threshold for voltage-dependent activation (V_{THR}) from the inspection of tail currents elicited by voltage steps in +20-mV increments, as described previously (Musset et al., 2008). The most negative voltage that generated I_{TAIL}, which was unambiguously larger than the background current, was designated as V_{THR}. Single-channel amplitudes were estimated by Gaussian fits to all-points histograms and direct inspection of single-channel records. Open probability (NP_{OPEN}) was computed by the equation $NP_{OPEN} = T_{OPEN}/T_{OPEN} + T_{CLOSED}$, where N is channel number, P_{OPEN} is open probability, T_{CLOSED} is total closed time, and T_{OPEN} is total open time, using Clampfit 9.2 (Axon Instruments). We selected patches with low basal channel activity for excised patch recordings.

Chemicals

2-APB, camphor, carvacrol, probenecid, allyl isothiocyanate, menthol, carbamylcholine (CCh), wortmannin (WM), phenylarsine oxide (PAO), BAPTA, EGTA, NMDG, and capsaicin were from Sigma-Aldrich. Ruthenium red was purchased from EMD. ATP was from Roche, purified bacterial phosphatidylinositol-specific PLC (PI-PLC) was obtained from Invitrogen, and diC8-PIPs and anti-$PI(4,5)P_2$ mouse monoclonal antiserum (mAb) were from Echelon Biosciences.

Online supplemental material

Fig. S1 shows current responses in primary human keratinocytes to various TRP channel agonists and compares the single-channel I-V relations of endogenous keratinocyte and expressed TRPV3 channels. Fig. S2 illustrates changes in the ligand, voltage, and temperature sensitivity that result from R696A and K705A mutations. Fig. S3 shows that R696A and K705A display reduced sensitivity to modulation of membrane $PI(4,5)P_2$ levels in cell-free membrane patches. The online supplemental material is available at http://www.jgp.org/cgi/content/full/jgp.200910388/DC1.

RESULTS

Endogenous TRPV3 currents in primary human keratinocytes are potentiated by $G_{q/11}$-coupled purinergic receptor activation

We measured membrane currents elicited by voltage steps in primary cultures of human epidermal keratinocytes using the whole cell voltage clamp mode and a Cs^+-based pipette solution that blocks most outward

K^+ channel current but permits measurement of outward conductances mediated by nonselective cation channels. Superfusion of the nonselective TRPV1-3 channel agonist 2-APB (30 µM) typically activated small voltage-dependent currents with steady-state outward rectification that reversed near 0 mV (Fig. 1, A and B). Carvacrol and camphor, but not capsaicin, probenecid, allyl isothiocyanate, or menthol, elicited currents with a similar steady-state I-V relation (Fig. S1), indicating that the observed currents were most likely a result of activation of TRPV3 and not TRPV1, TRPV2, TRPA1, or TRPM8 channels, respectively (Hu et al., 2004; Ständer et al., 2004; Bang et al., 2007; Facer et al., 2007; Anand et al., 2008). TRPV4 channels, which are also expressed in keratinocytes, are insensitive to 2-APB (Chung et al., 2004a). Ruthenium red, a voltage-dependent blocker of expressed TRPV3 and TRPV4 (Peier et al., 2002; Smith et al., 2002; Voets et al., 2002; Xu et al., 2002; Chung et al., 2004a), eliminated only the inward component of 2-APB–activated current, as expected (Fig. S1). The slope conductance of 2-APB–activated single-channel currents measured in inside-out membrane patches excised from primary keratinocytes (184.6 ± 2.1 pS) was close to that measured in patches from HM1 cells transfected with human TRPV3 cDNA (206.3 ± 1.6 pS; Fig. S1) under identical recording conditions. Collectively, these data indicate that the membrane currents measured under our experimental conditions in primary human keratinocytes are attributable to the expression of functional TRPV3 channels.

TRPV3 currents evoked by channel agonists such as 2-APB are potentiated by $G_{q/11}$-coupled receptor stimulation in HEK-293 cells (Xu et al., 2006), raising the question of whether native TRPV3 channels might be similarly modulated. We found that the amplitude of 2-APB–activated TRPV3 whole cell current in keratinocytes increased substantially (5.6 ± 1.6– and 6.3 ± 1.9–fold at +80 and −80 mV, respectively) after exposure to the purinergic P2Y receptor agonist ATP (Fig. 1, A, B, and E). P2Y stimulation also altered the voltage dependence of native TRPV3 currents, such that half-maximal activation ($V_{0.5}$) was shifted −61.7 ± 17.8 mV after exposure to ATP (Fig. 1, C, D, and F). In addition, the noninactivating portion of current increased substantially after ATP exposure (Fig. 1 C), and Boltzmann fits to the data clearly saturated at negative voltages, allowing us to

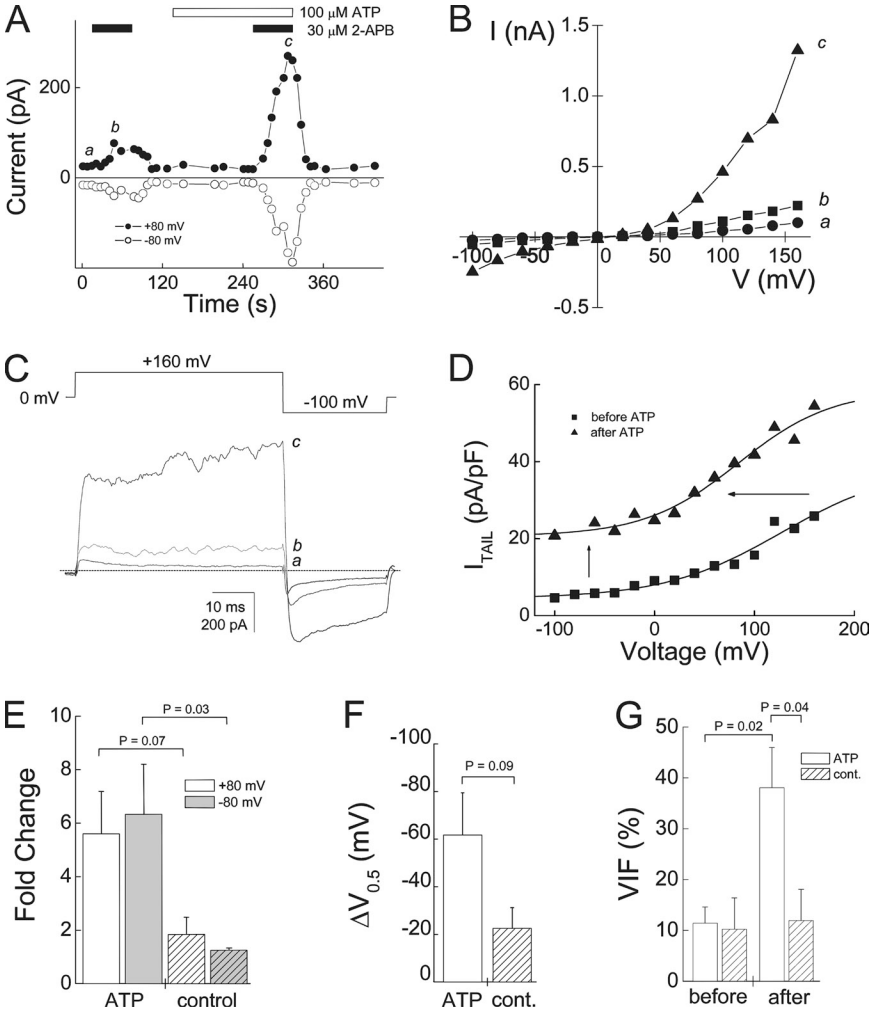

Figure 1. Endogenous TRPV3 currents in primary human keratinocytes are potentiated by $G_{q/11}$-coupled purinergic receptor activation. (A) Representative currents elicited by voltage steps to +80 mV (filled circles) or −80 mV (open circles) in the presence of 30 µM 2-APB (black bars) before and after exposure to 100 µM ATP (open bar). (B) Representative steady-state I-V relations taken at time points indicated in A: *a*, basal (circles); *b*, 30 µM 2-APB (squares); *c*, 30 µM 2-APB plus 100 µM ATP (triangles). (C) Representative currents (bottom) evoked by steps to the indicated voltage (top) at times *a*, *b*, and *c* indicated in A. Dashed line indicates the zero current level. (D) I_{TAIL}-V relation for voltage-dependent currents elicited in the presence of 2-APB before (squares) and after (triangles) exposure to ATP. Data are from the experiment shown in A, and lines represent fits to a Boltzmann function. Note that the midpoint of the Boltzmann fit ($V_{0.5}$) shifts negatively and I_{TAIL} at negative voltages (VIF) increases after ATP exposure. (E) Average change in step current at +80 mV (open bars) and −80 mV (shaded bars) after exposure to ATP (left) or vehicle control (right). (F) Average change in $V_{0.5}$ before and after ATP (open bar) or vehicle control (hatched bar) exposure. (G) Average VIF determined from the saturation of Boltzmann fits to I_{TAIL} at negative voltages before and after exposure to ATP (open bar) or vehicle control (hatched bar). For E–G, data represent means ± SEM from $n = 4$ cells.

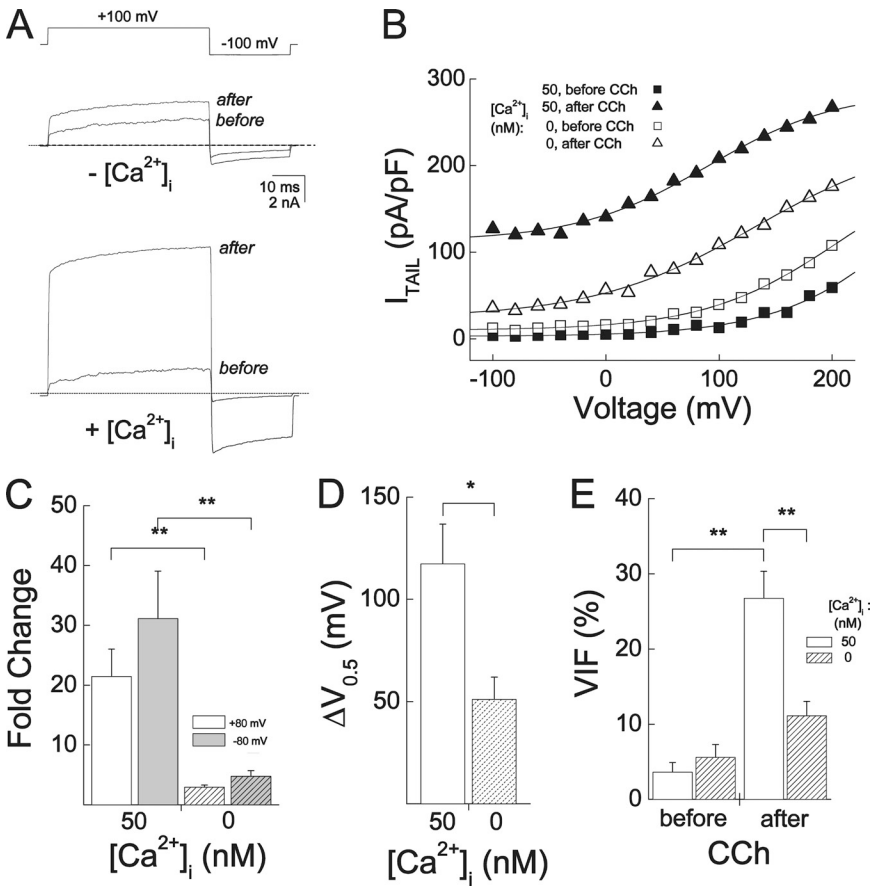

Figure 2. Potentiation of recombinant expressed TRPV3 currents by $G_{q/11}$-coupled muscarinic receptor activation. Whole cell currents were recorded from HM1 cells expressing WT TRPV3 under conditions that support (~50 nM of free $[Ca^{2+}]_i$) or prevent (free $[Ca^{2+}]_i$, <10 nM) PLCβ activity. (A) Representative current recordings elicited by voltage steps to +100 and −100 mV (upper panel, top) in the presence of 10 μM 2-APB before and after exposure to 100 μM CCh in the presence (lower panel) or absence (upper panel) of $[Ca^{2+}]$. Dashed lines indicate the zero current level. (B) I_{TAIL}–V relations for 2-APB–activated currents before (squares) and after (triangles) exposure to CCh in the presence (~50 nM $[Ca^{2+}]_i$; filled symbols) or absence (<10 nM $[Ca^{2+}]_i$; open symbols) of free Ca^{2+} in the pipette solution. Lines indicate fits to a Boltzmann function. (C) Average fold change in step current at +80 mV (white bars) and −80 mV (gray bars) after exposure to CCh in the presence (open bars) or absence (hatched bars) of $[Ca^{2+}]_i$. The average increase in TRPV3 current was 21.4 ± 4.5–fold at +80 mV (P = 0.0025) and 31.1 ± 7.9–fold at −80 mV (P = 0.0091). (D) Average change in $V_{0.5}$ before and after CCh in the presence (open bar) or absence (hatched bar) of $[Ca^{2+}]_i$ (P = 0.014). (E) Average VIF determined from Boltzmann fits before and after exposure to CCh in the presence (open bars) or absence (hatched bars) of $[Ca^{2+}]_i$ (P < 0.001, CCh + Ca^{2+} pre vs. post; P = 0.003, CCh + Ca^{2+} post vs. CCh − Ca^{2+} post). For C–E, data represent means ± SEM from n = 5–8 cells.

calculate the change in the voltage-independent fraction (VIF) of TRPV3. Voltage-independent conducting modes have been previously reported for several TRP channels, including TRPV3 (Chung et al., 2005). VIF increased 26.7 ± 5.1% after ATP exposure (Fig. 1, D and G), indicating that G_q-coupled receptor activation not only modulates the voltage dependence of TRPV3 channels but also causes a significant fraction of the current to remain constitutively open. The activation of purinergic P2Y receptors therefore appears sufficient to increase the amplitude of TRPV3 currents in keratinocytes by causing a shift in voltage-dependent activation toward

TABLE I

Effects of M_1 receptor stimulation and PI 4 kinase inhibition on TRPV3 channel activity

Treatment:		CCh (+Ca^{2+}_i)			CCh (−Ca^{2+}_i)			PAO		
DNA:		WT	R696A	K705A	WT	R696A	K705A	WT	R696A	K705A
Fold change	Mean	21.4	9.7	3.6[a]	2.9	4.0	1.5[a]	19.6	3.3[a]	1.5[a]
	SEM	1.6	3.3	0.3	0.4	0.6	0.1	5.6	1.0	0.1
$\Delta V_{0.5}$ (mV)	Mean	−117.3	−45.8[a]	−64.4[a]	−51.0	−35.1	−22.9	−109.9	−30.1[a]	−22.5[a]
	SEM	19.4	10.8	7.8	10.0	8.6	7.8	23.9	7.6	5.3
ΔVIF (%)	Mean	23.1	21.3	8.3[a]	5.5	24.0	1.3[a]	19.1	12.2	2.3[a]
	SEM	3.5	5.2	3.0	1.2	8.6	1.2	3.4	3.8	1.0
	n	8	6	7	7	4	6	8	5	8

Effects of M_1 stimulation (CCh) or PI 4 kinase inhibition (PAO) on current amplitude and voltage dependence for WT TRPV3, R696A, and K705A channels expressed in HM1 cells recorded with either 50 nM $[Ca^{2+}_i]$ (+) or <10 nM $[Ca^{2+}_i]$ (−) to control PLCβ activity. Currents were recorded in the presence of 10 μM (WT), 3 μM (R696A), or 6 μM (K705A) 2-APB at +80 mV. Final drug concentrations: 100 μM CCh and 30 μM PAO.
[a]P < 0.05 comparing WT TRPV3 and R696A or K705A, respectively.

negative membrane potentials and increasing the size of TRPV3 current that flows at voltages where channels are normally closed.

To examine the mechanism of $G_{q/11}$-coupled receptor potentiation of TRPV3 currents, we used the HM1 cell (Peralta et al., 1988) heterologous overexpression system that permits expression of recombinant TRPV3 channels together with recombinant human M_1 ACh receptors. In HM1 cells, the M_1 agonist CCh caused a larger potentiation of TRPV3 current amplitude (21.4- and 31.1-fold at +80 and −80 mV, respectively; Fig. 2, A and C, and Table I) than that seen in keratinocytes. The increased TRPV3 current amplitude and larger magnitude of $G_{q/11}$-coupled receptor responses in HM1 cells facilitated our analysis of changes in TRPV3 channel properties. As in keratinocytes, $G_{q/11}$-coupled receptor stimulation caused a large negative shift in $V_{0.5}$ (−117.3 ± 19.4 mV; Fig. 2, B and D, and Table I) and an increase in VIF (23.1 ± 3.5%; Fig. 2, B and E, and Table I).

To test whether M_1 modulation of TRPV3 required PLCβ activity, we omitted added Ca^{2+} from the BAPTA-buffered pipette solution, thereby reducing $[Ca^{2+}]_i$ from ∼50 to <10 nM (refer to Materials and methods). Lowering $[Ca^{2+}]_i$ to a similar extent was previously shown to inhibit PLCβ activity and abrogate M_1-dependent modulation of KCNQ2/3 channels expressed in HEK-293 cells (Horowitz et al., 2005). Blocking PLCβ by decreasing $[Ca^{2+}]_i$ largely abolished the CCh-induced increase in TRPV3 current amplitude, negative shift in $V_{0.5}$, and increase in VIF, but the effects of CCh were largely reversible on washout (Fig. 2 and Table I; not depicted). Activation of PLCβ by $G_{q/11}$-coupled receptor is therefore sufficient to rapidly amplify TRPV3 currents in both native and heterologous cellular contexts.

Stimulation of $G_{q/11}$-coupled receptors shifts TRPV3 agonist, voltage, and temperature sensitivity

In addition to modulating voltage-dependent activation of TRPV3, M_1 stimulation altered the potency for TRPV3 channel activation by the chemical agonist 2-APB, as indicated by an approximately fourfold increase in 2-APB potency after CCh exposure (Fig. 3 A). To determine

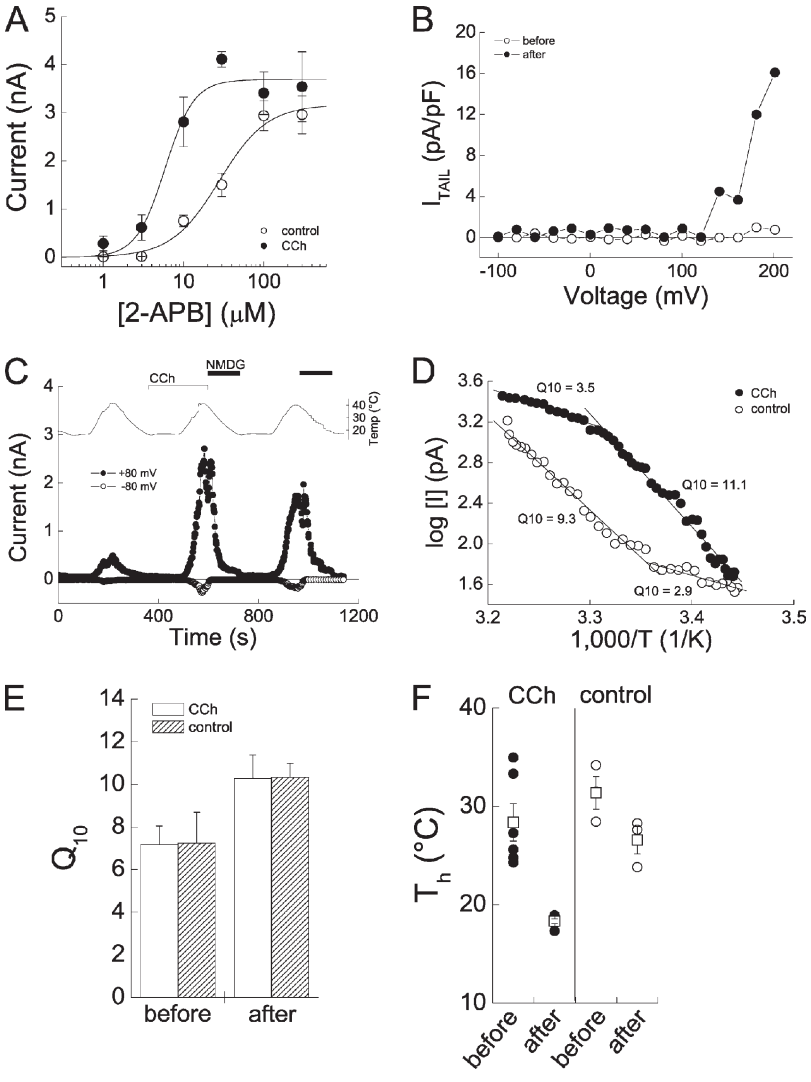

Figure 3. Stimulation of $G_{q/11}$-coupled receptors shifts TRPV3 agonist, voltage, and temperature sensitivity. (A) Concentration–response relation of 2-APB–activated currents recorded at +80 mV after exposure to either CCh (filled circles) or vehicle control (open circles). Solid lines represent fits to the Hill equation (CCh, EC_{50} = 6.7 ± 0.8 μM; vehicle control, EC_{50} = 28.6 ± 2.1 μM; n = 5 each). (B) Representative I_{TAIL}–V relation of tail currents (measured at −100 mV) elicited by steps to the indicated voltages before (open circles) and after (filled circles) exposure to CCh. Apparent V_{THR} shifted from >+200 mV before to +168.6 ± 9.6 mV (n = 7) after CCh exposure. (C) Representative currents at +80 mV (filled circles) or −80 mV (open circles) during repeated heating (17–40°C) in the absence or presence of CCh (open bar). The bath was superfused with NMDGCl (black bar) to check for inward leakage current after heating. (D) Representative temperature–current relations for heat-activated TRPV3 currents recorded in the presence of 100 μM CCh (filled circles) or vehicle control (open circles). Thermal coefficient (Q_{10}) values were determined from linear fits to each of two distinct phases of temperature-dependent activation. (E) Average Q_{10} values for temperature-dependent activation at +80 mV before and after exposure to either CCh (open bars) or vehicle control (hatched bars). (F) Apparent thermal threshold (T_h) for TRPV3 activation at +80 mV before and after exposure to CCh (filled circles; $P < 0.001$) or vehicle control (open circles). Open squares represent means ± SEM. For E and F, data represent means ± SEM from n = 3–7 cells.

whether $G_{q/11}$-coupled receptor modulation of TRPV3 activity requires channels to be simultaneously activated by the chemical agonist 2-APB, we measured voltage- and heat-activated currents before and after M_1 stimulation in cells that were naive to 2-APB exposure (Fig. 3). Before CCh, TRPV3 tail currents were not readily detectable (up to +200 mV); after CCh, we observed voltage-dependent activation of TRPV3 at ~+170 mV (Fig. 3 B and Table II). M_1 activation caused the apparent threshold for thermal activation (T_h) to shift −10°C (Fig. 3, C, D, and F), but the thermal coefficient (Q_{10}) was changed only slightly by CCh exposure (Fig. 3, D and E), suggesting that $G_{q/11}$-coupled receptor stimulation selectively affects the set point for thermal activation but not the fundamental mechanism of temperature sensing. Control recordings revealed only small and statistically insignificant changes in T_h and Q_{10} (Fig. 3, D–F). To rule out the possibility that heating induced a nonspecific leakage current, we superfused cells with NMDG at the peak of heat activation (Fig. 3 C). As expected, inward TRPV3 current was blocked, whereas outward currents were either unaffected or slightly potentiated (Xu et al., 2002; Chung et al., 2005). The sensitivity of TRPV3 channels to voltage, heating, and the chemical agonist 2-APB is therefore subject to modulation by receptor-catalyzed activation of PLCβ and increases the likelihood that channels will conduct current at typical skin temperature and resting membrane potential.

$PI(4,5)P_2$ depletion potentiates 2-APB–activated TRPV3 currents

Given that TRPV3 activity is positively modulated by $G_{q/11}$-coupled receptors and related TRP channels are regulated by $PI(4,5)P_2$, we wondered whether a PLCβ-catalyzed decrease in membrane $PI(4,5)P_2$ levels could account for the changes in TRPV3 properties that we observed. We therefore measured 2-APB–activated current before and after treating cells with drugs that block either PI 3 kinase (10 nM WM) or PI 4 kinase (30 µM PAO or 10 µM WM) (Nakanishi et al., 1995; Wiedemann et al., 1996; Várnai and Balla, 1998; Suh and Hille, 2007, 2008). PAO treatment resulted in a strong potentiation of TRPV3 current (19.6 ± 5.6–fold) that was similar to the effect of M_1 stimulation (Fig. 4, A and C, and Table I). Like CCh, PAO caused $V_{0.5}$ to shift −109.9 ± 23.9 mV and VIF to increase 19.1 ± 3.4% (Fig. 4, B, D, and E, and Table I). At 10 µM, the effect of WM on $V_{0.5}$ and VIF ($\Delta V_{0.5}$ = −98.4 ± 18.6 mV; ΔVIF = 19.7 ± 3.8%; n = 5) was similar to PAO, but the average current potentiation by 10 µM WM (9.6 ± 2.2– and 13.2 ± 2.8–fold increase at +80 and −80 mV, respectively) was less robust and failed to reach statistical significance (+80 mV, P = 0.06; −80 mV, P = 0.27; by Student's nonpaired t test). Although the data suggest that 30 µM PAO and 10 µM WM similarly affect TRPV3 activity by inhibiting PI 4 kinase, the effects of the two drugs at the concentrations tested are not identical. At a lower concentration (10 nM), the effect of WM was similar to vehicle control (Fig. 4, A–E), suggesting that PI 3 kinase activity is unlikely to participate in $G_{q/11}$-coupled receptor modulation of TRPV3 under our experimental conditions.

Combining PI 4 kinase inhibition (PAO) and CCh simulation resulted in greater current potentiation, a further negative shift in $V_{0.5}$, and a larger increase in VIF than was seen with either agent alone (Fig. 4). One possible explanation is that inhibiting $PI(4,5)P_2$ synthesis while simultaneously stimulating its hydrolysis more profoundly or persistently decreases the amount of plasma membrane $PI(4,5)P_2$, resulting in a larger effect on TRPV3 channels. Alternatively, the combined effect of CCh and PAO may

TABLE II

Effects of M_1 receptor stimulation on WT and mutant TRPV3 channel properties

		WT (before CCh)	WT (after CCh)	R696A	K705A
2-APB EC_{50} (µM)	Mean	28.6	6.7[a]	11.9[a]	14.6[a]
	SEM	2.1	0.8	1.0	2.1
	n	5	5	7	5
V_{THR} (mV)	Mean	>200	168.6	165.7	178.2
	SEM		9.6	11.3	5.7
	n	7	7	7	11
T_h (°C)	Mean	28.4	18.3[a]	22.9[a]	23.5[a]
	SEM	1.9	0.2	1.2	0.6
	n	6	6	7	6
Arrhenius slope	Mean	7.2	10.3	5.6	8.3
	SEM	0.9	1.1	0.5	0.4
	n	6	6	6	6

Effects of $G_{q/11}$ activation and TRP domain mutations on 2-APB potency (EC_{50}), apparent threshold for voltage-dependent activation (V_{THR}), apparent threshold for temperature-dependent activation (T_h), and Arrhenius slope of temperature-dependent activation for WT TRPV3, R696A, and K705A channels expressed in HM1 cells at +80 mV (except for V_{THR}).

[a]P < 0.05 compared to WT TRPV3 before CCh by Student's non-paired t test.

indicate that other signaling molecules downstream of M_1 activation, such as DAG, modulate TRPV3 activity. Collectively, our data suggest that depleting $PI(4,5)P_2$ is at least partially sufficient to modulate both voltage-dependent and voltage-independent activation of TRPV3 channels.

TRPV3 channel activity in excised patches is stimulated by $PI(4,5)P_2$ depletion

To more directly determine whether $PI(4,5)P_2$ is necessary for controlling basal TRPV3 channel activity, we treated excised inside-out patches with agents that are known to decrease membrane $PI(4,5)P_2$ levels (Suh and Hille, 2008). Spontaneous TRPV3 channel open probability (NP_{OPEN}) after patch excision was typically low (refer to Materials and methods), but the addition of the $PI(4,5)P_2$-scavenging mAb (Zhang et al., 2003; Albert et al., 2008; Suh and Hille, 2008) caused NP_{OPEN} to increase (NP_{OPEN} = 0.005 ± 0.002 before mAb; NP_{OPEN} = 0.64 ± 0.23 after mAb; Fig. 5, A–C). In contrast, control recordings showed only a negligible increase in NP_{OPEN} over the same 8-min incubation period (initial NP_{OPEN} = 0.015 ± 0.007; final NP_{OPEN} = 0.085 ± 0.055; Fig. 5, B and C). Purified bacterial PI-PLC (Sui et al., 1998; Suh and Hille, 2008) essentially mimicked the effect of mAb, causing TRPV3 channel activity to persistently increase (NP_{OPEN} = 0.021 ± 0.006 before PI-PLC; NP_{OPEN} = 0.89 ± 0.24 after PI-PLC; Fig. 5, B and C). In contrast to its effect on TRPC6 channels (Hofmann et al., 1999), the DAG analogue 1-oleoyl-2-acetyl-*sn*-glycerol (OAG; 100 µM) did not significantly increase TRPV3 channel activity (NP_{OPEN} = 0.025 ± 0.021 before OAG; NP_{OPEN} = 0.069 ± 0.031 after OAG; Fig. 5, B and C), suggesting that DAG production alone is not sufficient to potentiate TRPV3. Our results therefore suggest that depleting $PI(4,5)P_2$ increases the open probability of TRPV3 channels by sensitizing the channel to activation by other stimuli (i.e., thermal heating, membrane depolarization, and chemical agonists). $PI(4,5)P_2$ thus appears necessary to maintain tonic inhibition of TRPV3 channel activity under typical resting cellular conditions.

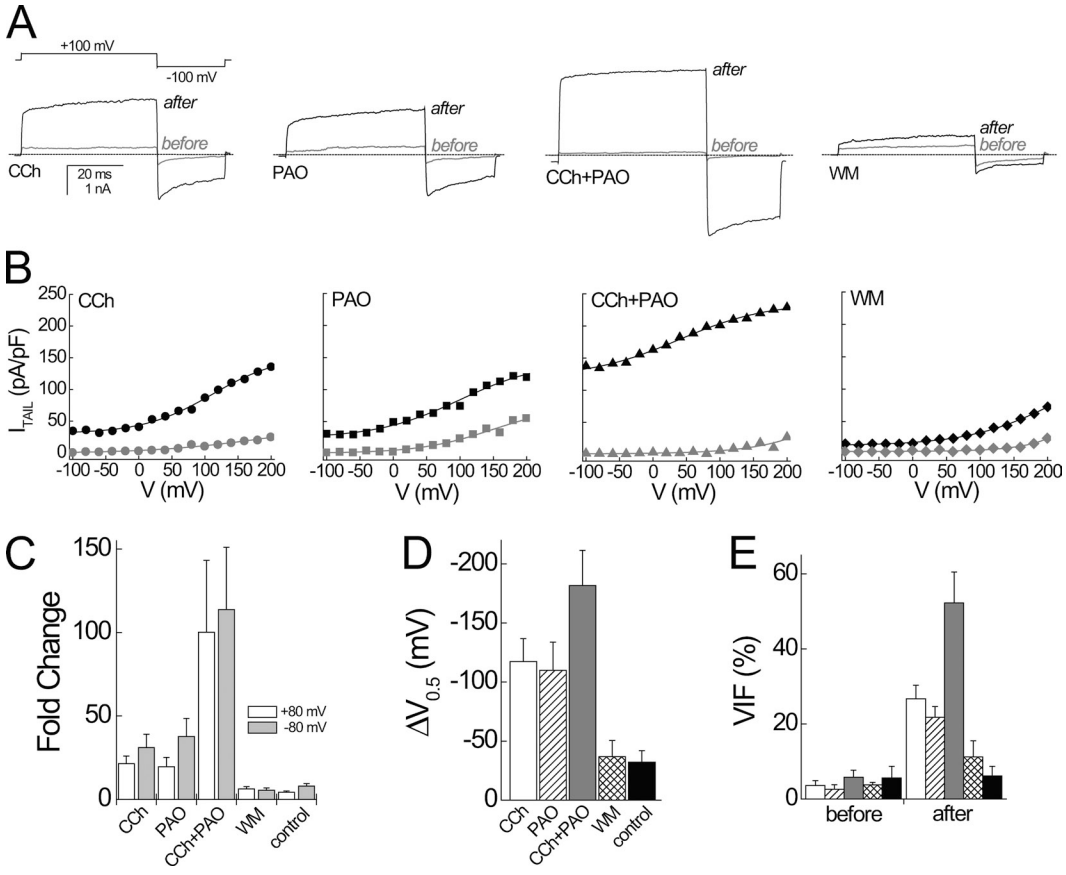

Figure 4. $PI(4,5)P_2$ depletion potentiates 2-APB–activated TRPV3 currents. HM1 cells expressing WT TRPV3 were treated for 2 min (CCh) or 5 min (PAO and WM) with the indicated drug, and currents were elicited in the presence of 10 µM 2-APB. (A) Representative currents resulting from voltage steps to +100 and −100 mV after treatment with the indicated drugs. (B) Representative I_{TAIL}–V relations from the same cells as current traces shown in A. (C) Average fold change in step current at +80 mV (open bars) and −80 mV (gray bars) elicited by treatment with the indicated drugs or vehicle control. (D and E) Average changes in $V_{0.5}$ (D) and VIF (E) under the indicated conditions. In D and E, bar shading represents CCh alone (open), PAO (diagonally hatched), CCh plus PAO (gray), WM (crosshatched), or vehicle control (black). Final drug concentrations in A–E: CCh, 100 µM; PAO, 30 µM; WM, 10 nM. For C–E, data represent means ± SEM from n = 5–8 cells. See Table I for a summary of the data.

To determine whether $PI(4,5)P_2$ was sufficient to decrease TRPV3 channel NP_{OPEN}, we applied a synthetic water-soluble analogue, diC8-$PI(4,5)P_2$ (dioctanoyl $PI(4,5)P_2$ or D-myo-phosphatidylinositol 4,5-bisphosphate C8) to the intracellular side of excised inside-out patches that had been previously treated with mAb or PI-PLC. Between 3 and 60 µM, diC8-$PI(4,5)P_2$ decreased PI-PLC–stimulated TRPV3 channel activity in a concentration-dependent fashion that was well fit to the Hill equation (IC_{50} = 10.0 ± 4.5 µM; n = 5 different patches; Fig. 6, A and D). Similar results were seen when TRPV3 channels were activated by $PI(4,5)P_2$ depletion with mAb (Fig. 6 C). TRPV3 activity rapidly returned after diC8-$PI(4,5)P_2$ washout in four of six patches, and the addition of either vehicle control or other diC8-phosphatidylinositol polyphosphates ($PI(3,4,5)P_3$ or $PI(3,5)P_2$) or monophosphates (PI(3)P, PI(4)P, or PI(5)P) at 30 µM failed to significantly decrease NP_{OPEN} (Fig. 6, B and E).

Although low concentrations (0.1–1 µM) of diC8-$PI(4,5)P_2$ sometimes appeared to stimulate TRPV3 activity relative to NP_{OPEN} measured after washout of $PI(4,5)P_2$-depleting agents (Fig. 6, A and D), this effect was inconsistent, and similar time-dependent changes in NP_{OPEN} after PI-PLC washout were also seen in some vehicle-treated patches (Fig. 6 B). A simple explanation for the data from excised patches is that TRPV3 activity is selectively inhibited by $PI(4,5)P_2$ in cell-free membrane patches.

Effects of mutating putative $PI(4,5)P_2$-binding residues in the TRP domain of TRPV3

To identify specific residues that are required for PLCβ- and $PI(4,5)P_2$-dependent modulation of TRPV3, we mutated two conserved basic residues in the TRP domain (R696A and K705A; Fig. 7 A) that had been previously identified as potential $PI(4,5)P_2$-interacting residues in TRPV1 and TRPV5 (Rohács et al., 2005; Brauchi et al., 2007). Both R696A and K705A expressed robust 2-APB–activated and voltage-dependent whole cell currents, but M_1-dependent channel modulation of

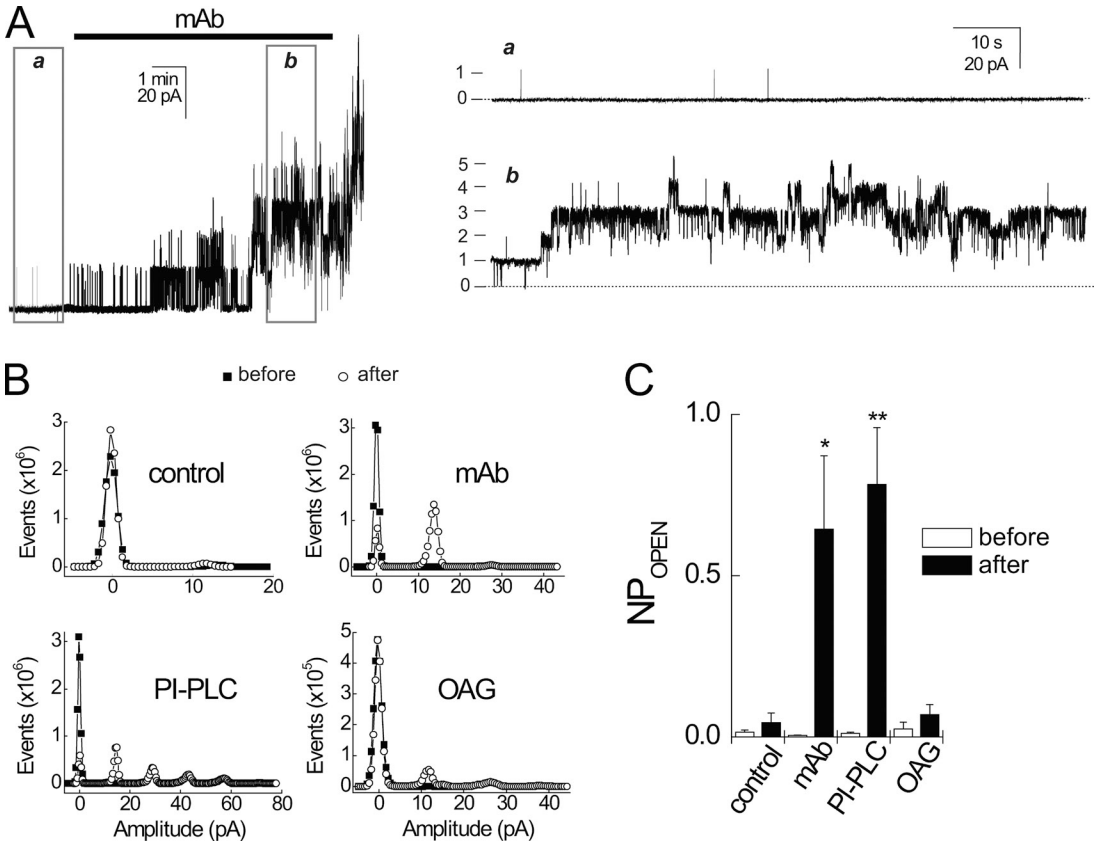

Figure 5. TRPV3 channel activity in excised patches is stimulated by $PI(4,5)P_2$ depletion. Inside-out patches pulled from HM1 cells expressing WT TRPV3 were exposed to either anti-$PI(4,5)P_2$ mAb or PI-PLC for 5 min, or OAG for 2 min (V_m = +80 mV). (A) A representative current record (left) showing the potentiating effect of mAb (1:200 dilution) on TRPV3 channel activity. Open boxes before (*a*) and after (*b*) reagent addition indicate time segments used for determination of NP_{OPEN}. Expanded current traces (right) during the time period shown in box *a* or *b*. The level of current associated with the indicated number of open TRPV3 channels is shown on the left. (B) Selected all-points histograms showing TRPV3 channel activity in patches before and after treatment with vehicle control, mAb (1:200 dilution; data from A), 100 µM OAG, or 0.5 U/ml PI-PLC. (C) Mean calculated NP_{OPEN} values before and after reagent addition in patches treated with vehicle control (n = 7), mAb (n = 7), OAG (n = 11), or PI-PLC (n = 29). Error bars represent SEM; *, $P < 0.05$; **, $P < 0.001$ versus control after vehicle addition by Student's nonpaired t test.

the mutant channels was attenuated compared with WT TRPV3 (Fig. 7 and Table I). Stimulation of M_1 by CCh caused 2-APB–activated current to increase only 9.7-fold and 3.6-fold in cells expressing R696A or K705A, respectively (Fig. 7, B, D, G, and I, and Table I), which was significantly less than the 21.4-fold potentiation seen for WT TRPV3 (Fig. 2). The CCh-induced negative shift in $V_{0.5}$ observed for WT TRPV3 was also significantly attenuated in both R696A and K705A (Fig. 7, C, E, H, and J, and Table I). Despite their similarity, some functional differences between R696A and K705A were noted. Whereas M_1 stimulation increased VIF of K705A channels only 8.3% in the presence of 50 nM $[Ca^{2+}]_i$ (compared with 23.1% for WT TRPV3), VIF increased 21.3% for R696A (Fig. 7 and Table I). Unlike WT TRPV3 and K705A, the increase in VIF for R696A appeared to be independent of $[Ca^{2+}]_i$ (Table I). The effects of neutralizing mutations at Arg696 and Lys705 support the hypothesis that TRP domain residues are required for the robust potentiation of TRPV3 channel activity resulting from receptor-mediated $PI(4,5)P_2$ hydrolysis or pharmacological depletion of $PI(4,5)P_2$.

R696 and K705 contribute to ligand, voltage, and temperature sensitivity in TRPV3

Because M_1 stimulation altered the sensitivity of WT TRPV3 to activation by 2-APB, voltage, and temperature (Fig. 3), and the R696A and K705A mutations were both much less sensitive to $G_{q/11}$-dependent modulation (Fig. 7 and Table I), we reasoned that both mutations might also affect 2-APB potency, voltage-dependent activation, and apparent thermal threshold. As summarized in Table II, 2-APB activated R696A and K705A currents approximately twofold more potently than it did WT TRPV3. V_{THR} measured in the absence of CCh was also more negative for both R696A and K705A than it was for WT TRPV3 (Table II and Fig. S2). In addition, T_h for R696A and K705A was shifted toward cooler temperatures compared with WT TRPV3 (Table II and Fig. S2). Interestingly, V_{THR},

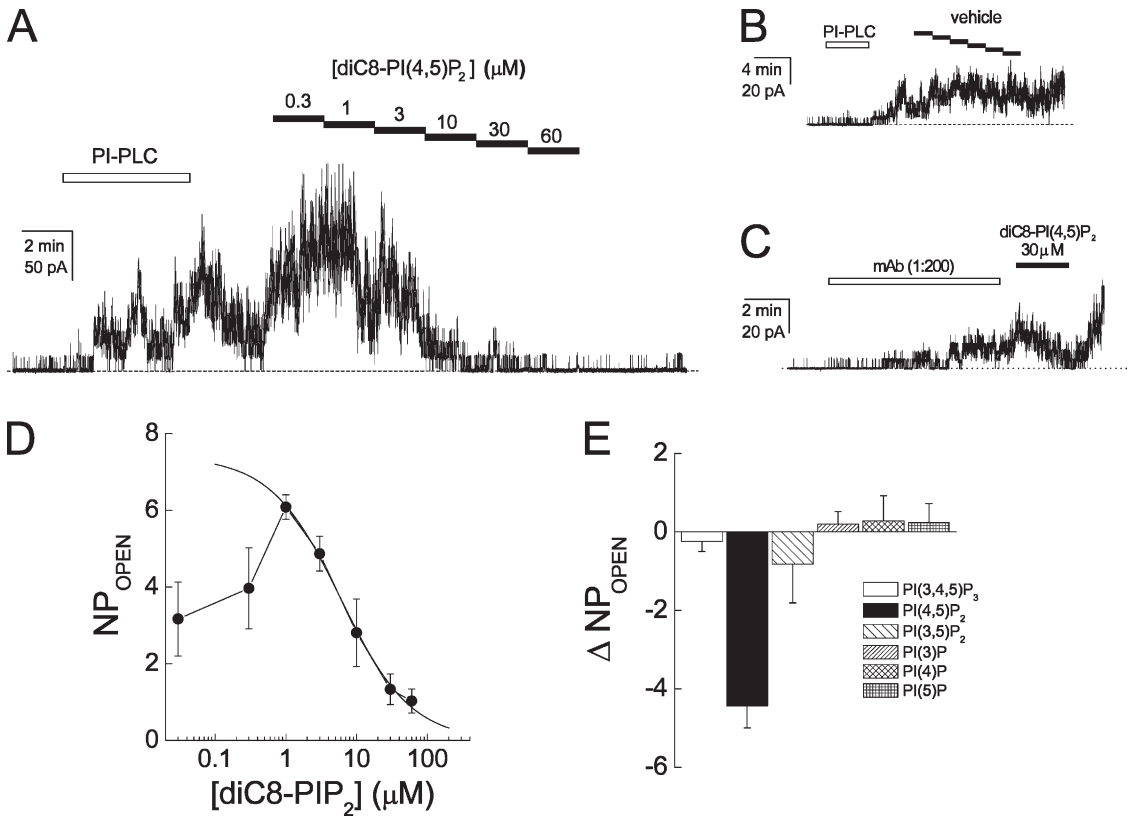

Figure 6. $PI(4,5)P_2$ decreases TRPV3 single-channel open probability. Inside-out patches excised from HM1 cells expressing WT TRPV3 (V_m = +80 mV) were treated with 0.5 U/ml PI-PLC (open bar), followed by water-soluble diC8-phosphatidylinositol phosphate analogues. (A and B) Representative current records showing the $[diC8\text{-}PI(4,5)P_2]$–dependent decrease in TRPV3 channel activity (A) and lack of similar effect in vehicle-treated patches (B). Filled bars in B represent serial dilutions of vehicle that mimic those used to achieve the indicated $[diC8\text{-}PI(4,5)P_2]$ shown in A. (C) A representative patch recording in which TRPV3 activity was stimulated by mAb and reversibly inhibited by 30 μM $diC8\text{-}PI(4,5)P_2$. (D) The average $diC8\text{-}PI(4,5)P_2$ concentration–response relation (data represent means ± SEM; n = 5 patches). Solid line represents a Hill fit to the data for 1–60 μM $diC8\text{-}PI(4,5)P_2$ (IC_{50} = 10.0 ± 4.5 μM). (E) Average change in NP_{OPEN} induced by the addition of the indicated diC8-phosphatidylinositol phosphates. Data represent means ± SEM from n = 3–6 patches.

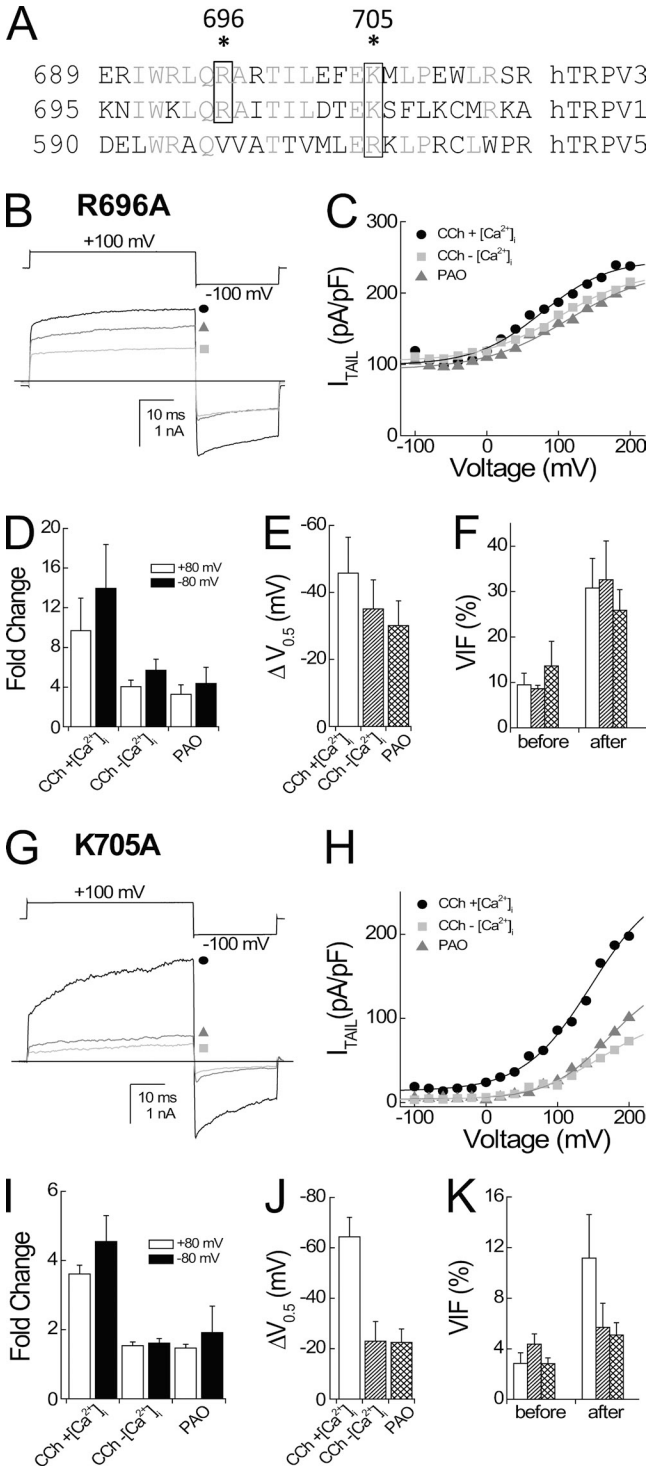

Figure 7. Effects of $G_{q/11}$-coupled receptor activation are attenuated in TRP domain mutants. (A) Sequence alignment of TRP domains from TRPV1, TRPV3, and TRPV5. Numbers indicate starting position in the amino acid sequence of human TRPV1 (NCBI Protein database accession no. NM_080705), human TRPV3 (AF514998.1), and human TRPV5 (NM_019841). Residues that are identical to TRPV3 are shown in gray, and basic residues previously identified as being important for $PI(4,5)P_2$-dependent modulation of TRPV1 and TRPV5 that are conserved in TRPV3 are shown within open boxes. Asterisks denote positions of TRPV3 mutations reported here. Whole cell currents were recorded from HM1 cells transfected with TRPV3 R696A (B–F) or K705A (G–K). M_1 was activated by bath application of 100 µM CCh in the presence (CCh + Ca^{2+}) or absence (CCh − Ca^{2+}) of buffered free $[Ca^{2+}]_i$, as described in Fig. 2. Cells were incubated with 30 µM PAO for 5 min between the first and second 2-APB applications to inhibit PI 4 kinase activity. The 2-APB concentrations used for R696A and K705A were 3 and 6 µM, respectively. (B and G) Representative current records (bottom) elicited by steps to the indicated voltages (top) recorded under the following conditions: CCh + Ca^{2+} (black circles), CCh − Ca^{2+} (gray squares), and PAO (gray triangles). The zero current level is indicated by a solid line. (C and H) Representative I_{TAIL}–V relations from the cells shown in B and G under the following conditions: CCh + Ca^{2+} (circles), CCh − Ca^{2+} (squares), and PAO (triangles). Lines represent fits to a Boltzmann function. (D and I) Average fold change in current amplitude at +80 mV (open bars) and −80 mV (black bars) elicited by treatment under the indicated conditions. (E and J) Average change in $V_{0.5}$ ($\Delta V_{0.5} = \Delta V_{0.5\ POST} - \Delta V_{0.5\ PRE}$) measured in cells treated under the indicated conditions. (F and K) Average change in VIF ($VIF_{POST} - VIF_{PRE}$) before and after treatment under the following conditions: CCh + Ca^{2+} (open bars), CCh − Ca^{2+} (diagonally hatched bars), and PAO (crosshatched bars). For D–F and I–K, data represent means ± SEM from $n = 5$–7 cells.

2-APB EC_{50}, and T_h values for R696A and K705A under resting conditions (i.e., without M_1 activation) were similar to those found for WT TRPV3 after $G_{q/11}$-dependent receptor stimulation (Table II), suggesting that these basic residues in the TRP domain contribute to the modulation of voltage, temperature, and chemical ligand sensitivity in TRPV3.

TRP domain–mutant channel activity is unaffected by $PI(4,5)P_2$ depletion

To determine whether the R696A and K705A mutations affected the sensitivity of TRPV3 to $PI(4,5)P_2$, we measured TRPV3 single-channel currents in excised patches treated with $PI(4,5)P_2$-depleting agents and diC8-$PI(4,5)P_2$. Spontaneous (basal) channel activity during the first 2 min after patch excision was sevenfold and 23-fold higher for R696A (NP_{OPEN} = 0.13 ± 0.06; Fig. 8, A–C) and K705A (NP_{OPEN} = 0.45 ± 0.10; Fig. 8, D–F), respectively, than for WT TRPV3 (basal NP_{OPEN} = 0.02 ± 0.004; Fig. 5). The single-channel conductances of R696A (175.5 ± 2.6 pS) and K705A (178.0 ± 3.2 pS) were similar to WT TRPV3 (180.8 ± 2.4 pS). The addition of either mAb or PI-PLC failed to cause a significant increase in NP_{OPEN} for either mutant compared with vehicle controls (Figs. 8 and S3). Likewise, R696A and K705A channel activity was unaffected by the addition of 30 µM diC8-$PI(4,5)P_2$ (Figs. 8, B and E, and S3), which exhibited a nearly maximal inhibitory effect on WT TRPV3 NP_{OPEN} (Fig. 6). Collectively, our findings indicate that TRPV3 channel activity is negatively regulated by resting $PI(4,5)P_2$ levels in the plasma membrane, and that basic residues in the TRP domain are essential for the effects of $PI(4,5)P_2$ on TRPV3.

DISCUSSION

Keratinocytes reside in close proximity to sensory nerve endings and leukocytes in skin, and bidirectional communication between different cell types is mediated by a variety of paracrine signaling molecules including G protein–coupled receptor agonists ATP, serotonin, histamine, prostaglandin E2, and leukotriene B4, and cytokines such as IL-1α, IL-6, IL-8, IL-17, IFN-γ, and TNF (Maurer et al., 1997; Corsini et al., 1998; Giustizieri et al., 2004; Koizumi et al., 2004; Lumpkin and Caterina, 2007; Huang et al., 2008; Zhu et al., 2009). Temperature-sensitive TRPV3 channels are highly expressed in keratinocytes, and thermal or mechanical stimulation of keratinocytes causes ATP release, which might cause autocrine stimulation of purinergic P2Y receptors (Peier et al., 2002; Smith et al., 2002; Xu et al., 2002; Koizumi et al., 2004; Inoue et al., 2007). ATP, histamine, and serotonin are known to generate a transient rise in $[Ca^{2+}]_i$ via receptor-mediated PLCβ activation and to stimulate keratinocyte proliferation, which is required for wound healing (Maurer et al., 1997; Lee et al., 2001; Giustizieri et al., 2004; Braun et al., 2006; Greig et al., 2008). TRPV3 current is potentiated by

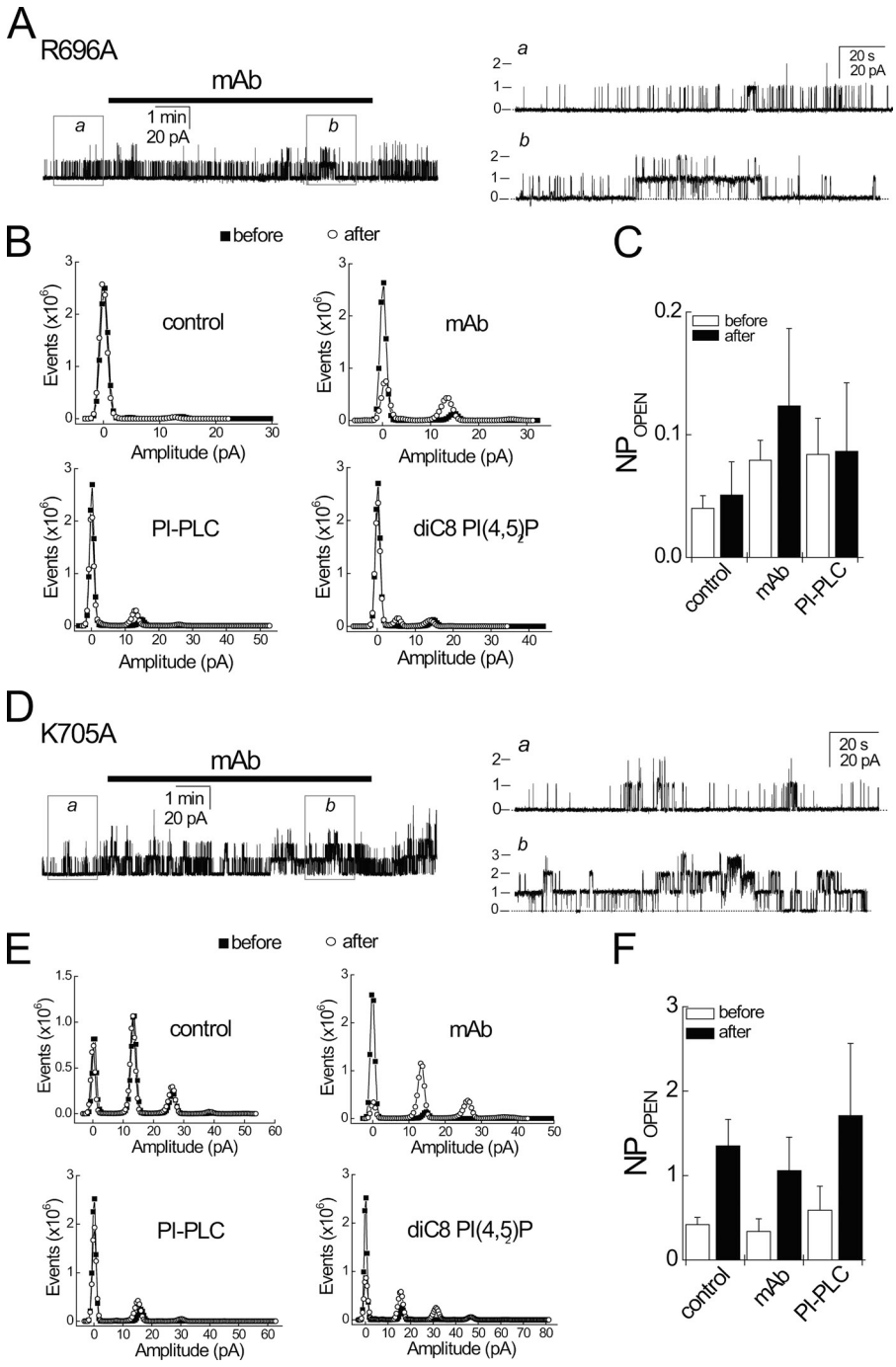

Figure 8. The TRP domain mutants R696A and K705A are insensitive to changes in $PI(4,5)P_2$. Inside-out patches were excised from HM1 cells expressing TRPV3 R696A or K705A, and voltage was clamped at +80 mV. (A and D) Representative current records from inside-out patches exposed to mAb (1:200 dilution; black bars, left). Open boxes indicate the time segments used for analysis of single-channel properties (*a*, before exposure to mAb; *b*, after exposure to mAb). Expanded current traces (right) during the time period shown in box *a* or *b*. (B and E) All-points histograms of raw data shown in A and D and similar recordings (see Fig. S3) in nontreated controls or patches treated with 0.5 U/ml PI-PLC and 30 μM diC8-$PI(4,5)P_2$. (C and F) Average NP_{OPEN} in patches expressing R696A or K705A either before (open bars) or after (black bars) the addition of mAb or PI-PLC, or in nontreated control recordings. Data represent means ± SEM from $n = 3$–5 patches.

$G_{q/11}$-coupled receptors in a heterologous overexpression system (Xu et al., 2006), suggesting that native TRPV3 channels could be subject to a similar regulatory mechanism in keratinocytes.

We show here that primary human keratinocytes express voltage- and agonist-evoked currents with biophysical and pharmacological properties that are strikingly similar to expressed TRPV3 channels. Extracellular ATP potentiated agonist-evoked TRPV3 current amplitude, shifted voltage-dependent activation toward negative potentials, and increased the proportion of voltage-independent current in both primary keratinocytes and HM1 cells, indicating that native and expressed TRPV3 channels are stimulated by similar mechanisms. The increased susceptibility to dermatitis and inflammatory skin lesions in hairless rodents bearing constitutively active TRPV3 channel mutations demonstrates that elevated TRPV3 activity is sufficient to dramatically alter skin health (Asakawa et al., 2006; Xiao et al., 2008b; Imura et al., 2009; Yoshioka et al., 2009). TRPV3 channels regulate growth factor receptor signaling and are required for TGF-α release (Cheng et al., 2010) and may also control the release of paracrine messengers (i.e., ATP, prostaglandin E2) from keratinocytes (Huang et al., 2008; Mandadi et al., 2009).

Consistent with previous reports describing activation mechanisms in TRPV1 and TRPM8 (Prescott and Julius, 2003; Rohács et al., 2005; Brauchi et al., 2007; Voets et al., 2007), we also found that the voltage, temperature, and agonist sensitivity of TRPV3 are coordinately modulated by $G_{q/11}$-coupled receptor stimulation. Both receptor-mediated PLCβ activation and pharmacological depletion of $PI(4,5)P_2$ were sufficient to cause a large negative shift in the voltage dependence of TRPV3 activation and increase the proportion of voltage-independent current. M_1 stimulation also increased the potency for 2-APB to activate TRPV3 current and shifted thermal activation toward cooler temperatures without significantly affecting Q_{10}. The inhibition of PI 4 kinase (but not PI 3 kinase) largely mimicked the M_1 effect, suggesting that CCh modulation of TRPV3 is primarily attributable to receptor-catalyzed hydrolysis of $PI(4,5)P_2$. Buffering $[Ca^{2+}]_i$ below 10 nM was previously demonstrated to prevent PLCβ-dependent modulation of KCNQ2/3 channels (Horowitz et al., 2005), and this maneuver also significantly attenuated the CCh-dependent effects on TRPV3 measured here.

DAG that is generated by PLCβ (and the PI-PLC used in excised patch recordings) may contribute to the increases in TRPV3 channel activity observed in some of our experiments. $PI(4,5)P_2$ and DAG were shown to coordinately regulate mammalian TRPC6 (Hofmann et al., 1999; Gudermann et al., 2004; Albert et al., 2008) and *Drosophila melanogaster* TRPL (Estacion et al., 2001) channel activities. However, a DAG analogue (OAG) failed to significantly elevate NP_{OPEN} in excised patches containing TRPV3 channels. In vitro depletion of $PI(4,5)P_2$ therefore appears to be sufficient to increase TRPV3 channel activity, but our data do not rule out the possibility that DAG (or other signaling molecules) generated by G_q-coupled receptor stimulation could also stimulate TRPV3 under different experimental conditions. Indeed, the synergistic effect of M_1 activation in cells pretreated with the PI 4 kinase inhibitor PAO is consistent with the possibility that another factor, possibly DAG, could increase TRPV3 current after $PI(4,5)P_2$ becomes depleted. Additional studies to elucidate other potentially important mechanisms of TRPV3 regulation are required. However, lowering $[PI(4,5)P_2]$ by the addition of mAb to inside-out patches was sufficient to increase TRPV3 channel activity, indicating that PLCβ activity is not a prerequisite for TRPV3 sensitization. We therefore conclude that TRPV3 channel activity is subject to negative regulation by resting levels of $PI(4,5)P_2$ in plasma membrane, such that the activation of $G_{q/11}$-coupled receptors leads to a rapid and dramatic increase in channel activity.

The large unitary conductance and high Ca^{2+} permeability of TRPV3 channels suggest that under physiological conditions, even a moderate elevation in TRPV3 channel opening is likely to have profound consequences for voltage- and Ca^{2+}-dependent cellular processes. Indeed, expression of constitutively active mutant TRPV3 channels or strong activation of related TRPV1 channels by capsaicin causes cell death both in vitro and in vivo (Sugimoto et al., 1998; Jin et al., 2005; Xiao et al., 2008b). Regulation of TRPV3 channel activity by PLC-coupled receptor-catalyzed $PI(4,5)P_2$ hydrolysis represents a plausible mechanism for maintaining strict control of basal channel activity under resting conditions while also allowing for rapid and reversible amplification of TRPV3 responses. TRPV3-mediated Ca^{2+} influx and depolarization thus allows for temporal and spatial control of signaling cascades that may control release of factors that are known to modulate inflammation, hair growth, keratinocyte differentiation, wound healing, and thermosensation (Braun et al., 2006; Lumpkin and Caterina, 2007; Greig et al., 2008; Cheng et al., 2010).

Changes in membrane $PI(4,5)P_2$ levels are known to modulate the activity of several TRP channels (Estacion et al., 2001; Runnels et al., 2002; Liu and Liman, 2003; Liu and Qin, 2005; Rohács et al., 2005; Nilius et al., 2006, 2008; Karashima et al., 2008; Otsuguro et al., 2008; Rohács, 2009; Mercado et al., 2010; Ufret-Vincenty et al., 2011). In a subset of TRP channels, basic residues in the TRP domain were proposed to mediate $PI(4,5)P_2$ binding (Nilius et al., 2008; Rohács, 2009). We found that TRPV3 channels are also sensitive to $PI(4,5)P_2$ in both whole cell and excised patch recording configurations and show here that neutralizing mutations of TRP domain residues R696 and K705 largely abrogate the

effects of techniques designed to reduce $PI(4,5)P_2$ levels in both whole cell and excised patch configurations. In addition, V_{THR}, T_h, and 2-APB potency values in R696A and K705A mimicked those seen for WT TRPV3 after M_1 activation, indicating that both residues are required for normal modulation of TRPV3 downstream of PLCβ. Elevated WT TRPV3 channel activity resulting from $PI(4,5)P_2$ depletion was reversed by the addition of water-soluble diC8-$PI(4,5)P_2$ with an IC_{50} of ∼10 µM. $PI(4,5)P_2$ therefore appears to modulate TRPV3 with potency comparable to other "high affinity" channels such as Kir2.1 (Huang et al., 1998; Kobrinsky et al., 2000). Despite exhibiting higher basal activities than WT TRPV3, both R696A and K705A mutants were insensitive to diC8-$PI(4,5)P_2$, suggesting that $PI(4,5)P_2$ could exert its effects on TRPV3 gating by directly interacting with these residues.

Electrostatic interactions between positively charged side chains of Arg and Lys residues and negatively charged phosphates on the inositol ring appear to be essential components of discrete $PI(4,5)P_2$-binding sites in a variety of ion channels and transporters (Rosenhouse-Dantsker and Logothetis, 2007; Suh and Hille, 2008). R696 and K705 in TRPV3 are homologous to conserved basic residues that are thought to participate in $PI(4,5)P_2$ interactions in several other TRP channels (Rohács et al., 2005; Brauchi et al., 2007). However, most of the tools commonly used to study ion channel interactions with PIPs do not directly measure lipid binding to functional channels under voltage control, and even excised membrane patches could include cytosolic enzymes that regulate lipid turnover and modulate channel activity. Although the effect of $PI(4,5)P_2$ on TRPV3 activity may therefore be indirect and require interactions with channel-associated $PI(4,5)P_2$-binding proteins (Suh and Hille, 2008), a recent report showed that the TRPV1-interacting and $PI(4,5)P_2$-binding protein Pirt is not required for channel activation by $PI(4,5)P_2$ (Ufret-Vincenty et al., 2011). Our data are consistent with the large body of experimental evidence indicating that PIP binding to basic residues directly regulates the activity of many ion channels and transporters (Rosenhouse-Dantsker and Logothetis, 2007; Suh and Hille, 2008; Ufret-Vincenty et al., 2011).

The rapid shift in TRPV3 voltage dependence that we observed after M_1 stimulation in HM1 cells or P2Y stimulation in keratinocytes is reminiscent of the effect of prolonged heating or exposure to high concentrations of channel agonists such as 2-APB (Chung et al., 2005). Previous studies concluded that both TRPV1 and TRPV3 channels undergo an apparently irreversible transition from voltage-dependent ("I1") to voltage-independent ("I2") conducting modes. Entry into I2 mode was shown to be accompanied by changes in T_h, 2-APB potency, and ion selectivity (Chung et al., 2005, 2008; Chen et al., 2009). Although transition to I2 is reported to be irreversible, we show that the activation of $G_{q/11}$-coupled receptors reversibly promotes occupancy of a voltage-independent TRPV3 gating mode that shares at least some properties with I2. Although detailed mechanistic explanations for agonist-, time-, and $PI(4,5)P_2$-dependent changes in TRPV3 gating require further investigation, studies on related TRP channels may provide some insight.

The voltage dependence of TRPM8, TRPA1, and TRPM4 is also subject to modulation by channel ligands, and under some circumstances, these channels also generate voltage-independent current (Zhang et al., 2005; Nilius et al., 2006; Matta and Ahern, 2007; Chen et al., 2009). Although the voltage-independent opening of TRP channels argues against an obligatory voltage-dependent transition in activation gating (Brauchi et al., 2007; Matta and Ahern, 2007; Nilius et al., 2007), it remains possible that voltage-independent current actually reflects a shift in voltage sensitivity to extremely negative potentials that are outside of the readily measurable range, using standard voltage clamp techniques (typically −200 to +200 mV). Nonetheless, $G_{q/11}$-coupled receptor modulation of TRPV3 leads to an increase in the probability that channels will generate current at the resting membrane potential, effectively abrogating the effect of hyperpolarizing voltage to induce channel closure.

The discovery of heat-insensitive but agonist- and voltage-sensitive TRPV3 pore domain mutants also demonstrates that voltage-dependent gating is separable from other modes of activation, at least in TRPV3 channels (Grandl et al., 2008). Residues in S4 and the S4–S5 linker of TRPM8 were reported to contribute to voltage sensitivity in TRPM8 (Voets et al., 2007), and point mutations of G573 in mouse TRPV3 that cause constitutive voltage-independent opening are also predicted to lie in the S4–S5 linker (Xiao et al., 2008b). The high resolution structure of a mammalian voltage-dependent K^+ channel suggests that voltage-dependent movement of S4 gating is coupled to pore opening via interactions between residues in the S4–S5 linker and C-terminal end of S6 (Long et al., 2007). The TRP domain is located at the intracellular end of S6, potentially placing it in proximity to the S4–S5 linker if basic channel architecture is similar in TRP channels and voltage-gated K^+ channels. Docking stimulations of a full atom–refined model of TRPV1 place the $PI(4,5)P_2$ polar head in position to interact with positive charges located in the TRP domain and the S4–S5 linker. Residues homologous to R696 and K705 lie on opposite sides of a putative $PI(4,5)P_2$-binding pocket and may differentially affect voltage sensing (Brauchi et al., 2007). Additional residues in the proximal C terminus could also be required for $PI(4,5)P_2$ binding in TRP channels (Ufret-Vincenty et al., 2011). The molecular determinants of voltage sensitivity and $PI(4,5)P_2$ binding may

therefore lie in close proximity, perhaps explaining the typically close coupling between voltage and lipid sensitivity (Nilius et al., 2007), and perhaps offering some insight into the differences in voltage-dependent gating between R696A and K705A observed here.

Unlike prototypical voltage-gated K^+ channels, in which voltage sensing is obligately coupled to channel opening, TRP channels appear to share more functional homology with Ca^{2+}-activated K^+ (BK) channels wherein voltage dependence is modulated by a ligand, $[Ca^{2+}]_i$ (Magleby, 2001; Horrigan and Aldrich, 2002; Bezanilla, 2008). A cogent and detailed understanding of gating mechanisms in polymodal TRPs and other channels activated by multiple stimuli will likely require a combination of high resolution protein structure, computer simulation, direct measurement of ligand–channel and lipid–channel interactions, and real-time electrophysiological analysis of channel function. Determining whether bound $PI(4,5)P_2$ directly participates in the formation or function of sensors for voltage, heat, and chemical ligands, or merely influences the function of other motifs that separately comprise sensors for various activation stimuli in TRPV3 and related channels, is a goal for future study.

In summary, we showed that native TRPV3 channels in primary human keratinocytes and recombinant TRPV3 channels expressed in HEK-293 cells are strongly modulated by stimulation of $G_{q/11}$-coupled receptors. PLCβ-catalyzed hydrolysis of $PI(4,5)P_2$ accounts for most of the observed effects on TRPV3 channel activity: (a) a potentiation of current amplitude that is driven by a negative shift in the voltage dependence of opening and an increase in the fraction of channels that conduct in a voltage-independent mode; and (b) a decrease in the apparent threshold for thermal activation. Each of these effects will tend to increase the likelihood that TRPV3 channels will be open under physiological conditions. Two basic residues in the TRP domain are required for $G_{q/11}$-coupled receptor modulation of TRPV3 and could participate in $PI(4,5)P_2$ binding. We hypothesize that $PI(4,5)P_2$-bound TRPV3 channels open only rarely and that PLC activity or $PI(4,5)P_2$ depletion provides relief of tonic inhibition. $PI(4,5)P_2$ thus appears well suited to regulate TRPV3 channel activity in vivo and thereby control Ca^{2+}-dependent cellular signaling in keratinocytes or other cells expressing TRPV3.

The authors wish to thank David Clapham for generous support; Nat Blair, Vasileous Petrou, and Carlos A. Villalba-Galea for insightful discussions; and Harald Bartel and Thomas Lichtleitner for technical assistance. The authors are grateful to Professors Steinstraesser and Steinau for providing human keratinocytes and would like to thank Heike Benecke for assistance with keratinocyte culture.

This work was supported by National Institutes of Health training grant HLO7572 (to the Department of Pediatrics, Children's Hospital Boston; I.S. Ramsey) and the International Max-Planck Research School in Chemical Biology (to J.F. Doerner).

Angus C. Nairn served as editor.

Submitted: 21 December 2009
Accepted: 27 January 2011

REFERENCES

Albert, A.P., S.N. Saleh, and W.A. Large. 2008. Inhibition of native TRPC6 channel activity by phosphatidylinositol 4,5-bisphosphate in mesenteric artery myocytes. *J. Physiol.* 586:3087–3095. doi:10.1113/jphysiol.2008.153676

Anand, U., W.R. Otto, P. Facer, N. Zebda, I. Selmer, M.J. Gunthorpe, I.P. Chessell, M. Sinisi, R. Birch, and P. Anand. 2008. TRPA1 receptor localisation in the human peripheral nervous system and functional studies in cultured human and rat sensory neurons. *Neurosci. Lett.* 438:221–227. doi:10.1016/j.neulet.2008.04.007

Asakawa, M., T. Yoshioka, T. Matsutani, I. Hikita, M. Suzuki, I. Oshima, K. Tsukahara, A. Arimura, T. Horikawa, T. Hirasawa, and T. Sakata. 2006. Association of a mutation in TRPV3 with defective hair growth in rodents. *J. Invest. Dermatol.* 126:2664–2672. doi:10.1038/sj.jid.5700468

Bang, S., K.Y. Kim, S. Yoo, S.H. Lee, and S.W. Hwang. 2007. Transient receptor potential V2 expressed in sensory neurons is activated by probenecid. *Neurosci. Lett.* 425:120–125. doi:10.1016/j.neulet.2007.08.035

Bezanilla, F. 2008. Ion channels: from conductance to structure. *Neuron.* 60:456–468. doi:10.1016/j.neuron.2008.10.035

Brauchi, S., G. Orta, C. Mascayano, M. Salazar, N. Raddatz, H. Urbina, E. Rosenmann, F. Gonzalez-Nilo, and R. Latorre. 2007. Dissection of the components for PIP_2 activation and thermosensation in TRP channels. *Proc. Natl. Acad. Sci. USA.* 104:10246–10251. doi:10.1073/pnas.0703420104

Braun, M., K. Lelieur, and M. Kietzmann. 2006. Purinergic substances promote murine keratinocyte proliferation and enhance impaired wound healing in mice. *Wound Repair Regen.* 14:152–161. doi:10.1111/j.1743-6109.2006.00105.x

Chen, J., D. Kim, B.R. Bianchi, E.J. Cavanaugh, C.R. Faltynek, P.R. Kym, and R.M. Reilly. 2009. Pore dilation occurs in TRPA1 but not in TRPM8 channels. *Mol. Pain.* 5:3. doi:10.1186/1744-8069-5-3

Cheng, X., J. Jin, L. Hu, D. Shen, X.P. Dong, M.A. Samie, J. Knoff, B. Eisinger, M.L. Liu, S.M. Huang, et al. 2010. TRP channel regulates EGFR signaling in hair morphogenesis and skin barrier formation. *Cell.* 141:331–343. doi:10.1016/j.cell.2010.03.013

Chuang, H.H., E.D. Prescott, H. Kong, S. Shields, S.E. Jordt, A.I. Basbaum, M.V. Chao, and D. Julius. 2001. Bradykinin and nerve growth factor release the capsaicin receptor from PtdIns(4,5)P_2-mediated inhibition. *Nature.* 411:957–962. doi:10.1038/35082088

Chung, M.K., H. Lee, and M.J. Caterina. 2003. Warm temperatures activate TRPV4 in mouse 308 keratinocytes. *J. Biol. Chem.* 278:32037–32046. doi:10.1074/jbc.M303251200

Chung, M.K., H. Lee, A. Mizuno, M. Suzuki, and M.J. Caterina. 2004a. 2-aminoethoxydiphenyl borate activates and sensitizes the heat-gated ion channel TRPV3. *J. Neurosci.* 24:5177–5182. doi:10.1523/JNEUROSCI.0934-04.2004

Chung, M.K., H. Lee, A. Mizuno, M. Suzuki, and M.J. Caterina. 2004b. TRPV3 and TRPV4 mediate warmth-evoked currents in primary mouse keratinocytes. *J. Biol. Chem.* 279:21569–21575. doi:10.1074/jbc.M401872200

Chung, M.K., A.D. Güler, and M.J. Caterina. 2005. Biphasic currents evoked by chemical or thermal activation of the heat-gated ion channel, TRPV3. *J. Biol. Chem.* 280:15928–15941. doi:10.1074/jbc.M500596200

Chung, M.K., A.D. Güler, and M.J. Caterina. 2008. TRPV1 shows dynamic ionic selectivity during agonist stimulation. *Nat. Neurosci.* 11:555–564. doi:10.1038/nn.2102

Clapham, D.E. 2003. TRP channels as cellular sensors. *Nature.* 426:517–524. doi:10.1038/nature02196

Corsini, E., A. Primavera, M. Marinovich, and C.L. Galli. 1998. Selective induction of cell-associated interleukin-1α in murine keratinocytes by chemical allergens. *Toxicology.* 129:193–200. doi:10.1016/S0300-483X(98)00088-2

Estacion, M., W.G. Sinkins, and W.P. Schilling. 2001. Regulation of Drosophila transient receptor potential-like (TrpL) channels by phospholipase C-dependent mechanisms. *J. Physiol.* 530:1–19. doi:10.1111/j.1469-7793.2001.0001m.x

Facer, P., M.A. Casula, G.D. Smith, C.D. Benham, I.P. Chessell, C. Bountra, M. Sinisi, R. Birch, and P. Anand. 2007. Differential expression of the capsaicin receptor TRPV1 and related novel receptors TRPV3, TRPV4 and TRPM8 in normal human tissues and changes in traumatic and diabetic neuropathy. *BMC Neurol.* 7:11. doi:10.1186/1471-2377-7-11

Gamper, N., and M.S. Shapiro. 2007. Regulation of ion transport proteins by membrane phosphoinositides. *Nat. Rev. Neurosci.* 8:921–934. doi:10.1038/nrn2257

Giustizieri, M.L., C. Albanesi, J. Fluhr, P. Gisondi, J. Norgauer, and G. Girolomoni. 2004. H1 histamine receptor mediates inflammatory responses in human keratinocytes. *J. Allergy Clin. Immunol.* 114:1176–1182. doi:10.1016/j.jaci.2004.07.054

Grandl, J., H. Hu, M. Bandell, B. Bursulaya, M. Schmidt, M. Petrus, and A. Patapoutian. 2008. Pore region of TRPV3 ion channel is specifically required for heat activation. *Nat. Neurosci.* 11:1007–1013. doi:10.1038/nn.2169

Greig, A.V., C. Linge, and G. Burnstock. 2008. Purinergic receptors are part of a signalling system for proliferation and differentiation in distinct cell lineages in human anagen hair follicles. *Purinergic Signal.* 4:331–338. doi:10.1007/s11302-008-9108-0

Gudermann, T., T. Hofmann, M. Mederos y Schnitzler, and A. Dietrich. 2004. Activation, subunit composition and physiological relevance of DAG-sensitive TRPC proteins. *Novartis Found. Symp.* 258:103–118. doi:10.1002/0470862580.ch8

Ho, S.N., H.D. Hunt, R.M. Horton, J.K. Pullen, and L.R. Pease. 1989. Site-directed mutagenesis by overlap extension using the polymerase chain reaction. *Gene.* 77:51–59. doi:10.1016/0378-1119(89)90358-2

Hofmann, T., A.G. Obukhov, M. Schaefer, C. Harteneck, T. Gudermann, and G. Schultz. 1999. Direct activation of human TRPC6 and TRPC3 channels by diacylglycerol. *Nature.* 397:259–263. doi:10.1038/16711

Horowitz, L.F., W. Hirdes, B.C. Suh, D.W. Hilgemann, K. Mackie, and B. Hille. 2005. Phospholipase C in living cells: activation, inhibition, Ca^{2+} requirement, and regulation of M current. *J. Gen. Physiol.* 126:243–262. doi:10.1085/jgp.200509309

Horrigan, F.T., and R.W. Aldrich. 2002. Coupling between voltage sensor activation, Ca^{2+} binding and channel opening in large conductance (BK) potassium channels. *J. Gen. Physiol.* 120:267–305. doi:10.1085/jgp.20028605

Hu, H.Z., Q. Gu, C. Wang, C.K. Colton, J. Tang, M. Kinoshita-Kawada, L.Y. Lee, J.D. Wood, and M.X. Zhu. 2004. 2-aminoethoxydiphenyl borate is a common activator of TRPV1, TRPV2, and TRPV3. *J. Biol. Chem.* 279:35741–35748. doi:10.1074/jbc.M404164200

Hu, H.Z., R. Xiao, C. Wang, N. Gao, C.K. Colton, J.D. Wood, and M.X. Zhu. 2006. Potentiation of TRPV3 channel function by unsaturated fatty acids. *J. Cell. Physiol.* 208:201–212. doi:10.1002/jcp.20648

Huang, C.L., S. Feng, and D.W. Hilgemann. 1998. Direct activation of inward rectifier potassium channels by PIP_2 and its stabilization by Gbetagamma. *Nature.* 391:803–806. doi:10.1038/35882

Huang, S.M., H. Lee, M.K. Chung, U. Park, Y.Y. Yu, H.B. Bradshaw, P.A. Coulombe, J.M. Walker, and M.J. Caterina. 2008. Overexpressed transient receptor potential vanilloid 3 ion channels in skin keratinocytes modulate pain sensitivity via prostaglandin E_2. *J. Neurosci.* 28:13727–13737. doi:10.1523/JNEUROSCI.5741-07.2008

Imura, K., T. Yoshioka, T. Hirasawa, and T. Sakata. 2009. Role of TRPV3 in immune response to development of dermatitis. *J. Inflamm. (Lond.).* 6:17. doi:10.1186/1476-9255-6-17

Inoue, K., J. Hosoi, and M. Denda. 2007. Extracellular ATP has stimulatory effects on the expression and release of IL-6 via purinergic receptors in normal human epidermal keratinocytes. *J. Invest. Dermatol.* 127:362–371. doi:10.1038/sj.jid.5700526

Jacobsen, F., D. Mittler, T. Hirsch, A. Gerhards, M. Lehnhardt, B. Voss, H.U. Steinau, and L. Steinstraesser. 2005. Transient cutaneous adenoviral gene therapy with human host defense peptide hCAP-18/LL-37 is effective for the treatment of burn wound infections. *Gene Ther.* 12:1494–1502. doi:10.1038/sj.gt.3302568

Jin, H.W., H. Ichikawa, M. Fujita, T. Yamaai, K. Mukae, K. Nomura, and T. Sugimoto. 2005. Involvement of caspase cascade in capsaicin-induced apoptosis of dorsal root ganglion neurons. *Brain Res.* 1056:139–144. doi:10.1016/j.brainres.2005.07.025

Karashima, Y., J. Prenen, V. Meseguer, G. Owsianik, T. Voets, and B. Nilius. 2008. Modulation of the transient receptor potential channel TRPA1 by phosphatidylinositol 4,5-biphosphate manipulators. *Pflugers Arch.* 457:77–89. doi:10.1007/s00424-008-0493-6

Kobrinsky, E., T. Mirshahi, H. Zhang, T. Jin, and D.E. Logothetis. 2000. Receptor-mediated hydrolysis of plasma membrane messenger PIP_2 leads to K^+-current desensitization. *Nat. Cell Biol.* 2:507–514. doi:10.1038/35019544

Koizumi, S., K. Fujishita, K. Inoue, Y. Shigemoto-Mogami, M. Tsuda, and K. Inoue. 2004. Ca^{2+} waves in keratinocytes are transmitted to sensory neurons: the involvement of extracellular ATP and P2Y2 receptor activation. *Biochem. J.* 380:329–338. doi:10.1042/BJ20031089

Lee, H., and M.J. Caterina. 2005. TRPV channels as thermosensory receptors in epithelial cells. *Pflugers Arch.* 451:160–167. doi:10.1007/s00424-005-1438-y

Lee, W.K., S.W. Choi, H.R. Lee, E.J. Lee, K.H. Lee, and H.O. Kim. 2001. Purinoceptor-mediated calcium mobilization and proliferation in HaCaT keratinocytes. *J. Dermatol. Sci.* 25:97–105. doi:10.1016/S0923-1811(00)00117-1

Liu, D., and E.R. Liman. 2003. Intracellular Ca^{2+} and the phospholipid PIP2 regulate the taste transduction ion channel TRPM5. *Proc. Natl. Acad. Sci. USA.* 100:15160–15165. doi:10.1073/pnas.2334159100

Liu, B., and F. Qin. 2005. Functional control of cold- and menthol-sensitive TRPM8 ion channels by phosphatidylinositol 4,5-bisphosphate. *J. Neurosci.* 25:1674–1681. doi:10.1523/JNEUROSCI.3632-04.2005

Long, S.B., X. Tao, E.B. Campbell, and R. MacKinnon. 2007. Atomic structure of a voltage-dependent K^+ channel in a lipid membrane-like environment. *Nature.* 450:376–382. doi:10.1038/nature06265

Lukacs, V., B. Thyagarajan, P. Varnai, A. Balla, T. Balla, and T. Rohács. 2007. Dual regulation of TRPV1 by phosphoinositides. *J. Neurosci.* 27:7070–7080. doi:10.1523/JNEUROSCI.1866-07.2007

Lumpkin, E.A., and M.J. Caterina. 2007. Mechanisms of sensory transduction in the skin. *Nature.* 445:858–865. doi:10.1038/nature05662

Magleby, K.L. 2001. Kinetic gating mechanisms for BK channels: when complexity leads to simplicity. *J. Gen. Physiol.* 118:583–587. doi:10.1085/jgp.118.5.583

Mandadi, S., T. Sokabe, K. Shibasaki, K. Katanosaka, A. Mizuno, A. Moqrich, A. Patapoutian, T. Fukumi-Tominaga, K. Mizumura, and M. Tominaga. 2009. TRPV3 in keratinocytes transmits temperature information to sensory neurons via ATP. *Pflugers Arch.* 458:1093–1102. doi:10.1007/s00424-009-0703-x

Matta, J.A., and G.P. Ahern. 2007. Voltage is a partial activator of rat thermosensitive TRP channels. *J. Physiol.* 585:469–482. doi:10.1113/jphysiol.2007.144287

Maurer, M., M. Opitz, B.M. Henz, and R. Paus. 1997. The mast cell products histamine and serotonin stimulate and TNF-alpha inhibits the proliferation of murine epidermal keratinocytes in situ. *J. Dermatol. Sci.* 16:79–84. doi:10.1016/S0923-1811(97)00043-1

Mercado, J., A. Gordon-Shaag, W.N. Zagotta, and S.E. Gordon. 2010. Ca^{2+}-dependent desensitization of TRPV2 channels is mediated by hydrolysis of phosphatidylinositol 4,5-bisphosphate. *J. Neurosci.* 30:13338–13347. doi:10.1523/JNEUROSCI.2108-10.2010

Montell, C. 2001. Physiology, phylogeny, and functions of the TRP superfamily of cation channels. *Sci. STKE.* 2001:re1. doi:10.1126/stke.2001.90.re1

Moqrich, A., S.W. Hwang, T.J. Earley, M.J. Petrus, A.N. Murray, K.S. Spencer, M. Andahazy, G.M. Story, and A. Patapoutian. 2005. Impaired thermosensation in mice lacking TRPV3, a heat and camphor sensor in the skin. *Science.* 307:1468–1472. doi:10.1126/science.1108609

Musset, B., V.V. Cherny, D. Morgan, Y. Okamura, I.S. Ramsey, D.E. Clapham, and T.E. DeCoursey. 2008. Detailed comparison of expressed and native voltage-gated proton channel currents. *J. Physiol.* 586:2477–2486. doi:10.1113/jphysiol.2007.149427

Nakanishi, S., K.J. Catt, and T. Balla. 1995. A wortmannin-sensitive phosphatidylinositol 4-kinase that regulates hormone-sensitive pools of inositolphospholipids. *Proc. Natl. Acad. Sci. USA.* 92:5317–5321. doi:10.1073/pnas.92.12.5317

Nilius, B. 2007. TRP channels in disease. *Biochim. Biophys. Acta.* 1772:805–812.

Nilius, B., F. Mahieu, J. Prenen, A. Janssens, G. Owsianik, R. Vennekens, and T. Voets. 2006. The Ca^{2+}-activated cation channel TRPM4 is regulated by phosphatidylinositol 4,5-biphosphate. *EMBO J.* 25:467–478. doi:10.1038/sj.emboj.7600963

Nilius, B., F. Mahieu, Y. Karashima, and T. Voets. 2007. Regulation of TRP channels: a voltage-lipid connection. *Biochem. Soc. Trans.* 35:105–108. doi:10.1042/BST0350105

Nilius, B., G. Owsianik, and T. Voets. 2008. Transient receptor potential channels meet phosphoinositides. *EMBO J.* 27:2809–2816. doi:10.1038/emboj.2008.217

Otsuguro, K., J. Tang, Y. Tang, R. Xiao, M. Freichel, V. Tsvilovskyy, S. Ito, V. Flockerzi, M.X. Zhu, and A.V. Zholos. 2008. Isoform-specific inhibition of TRPC4 channel by phosphatidylinositol 4,5-bisphosphate. *J. Biol. Chem.* 283:10026–10036. doi:10.1074/jbc.M707306200

Peier, A.M., A.J. Reeve, D.A. Andersson, A. Moqrich, T.J. Earley, A.C. Hergarden, G.M. Story, S. Colley, J.B. Hogenesch, P. McIntyre, et al. 2002. A heat-sensitive TRP channel expressed in keratinocytes. *Science.* 296:2046–2049. doi:10.1126/science.1073140

Peralta, E.G., A. Ashkenazi, J.W. Winslow, J. Ramachandran, and D.J. Capon. 1988. Differential regulation of PI hydrolysis and adenylyl cyclase by muscarinic receptor subtypes. *Nature.* 334:434–437. doi:10.1038/334434a0

Phelps, C.B., R.R. Wang, S.S. Choo, and R. Gaudet. 2010. Differential regulation of TRPV1, TRPV3, and TRPV4 sensitivity through a conserved binding site on the ankyrin repeat domain. *J. Biol. Chem.* 285:731–740. doi:10.1074/jbc.M109.052548

Prescott, E.D., and D. Julius. 2003. A modular PIP2 binding site as a determinant of capsaicin receptor sensitivity. *Science.* 300:1284–1288. doi:10.1126/science.1083646

Ramsey, I.S., M. Delling, and D.E. Clapham. 2006. An introduction to TRP channels. *Annu. Rev. Physiol.* 68:619–647. doi:10.1146/annurev.physiol.68.040204.100431

Rohács, T. 2009. Phosphoinositide regulation of non-canonical transient receptor potential channels. *Cell Calcium.* 45:554–565. doi:10.1016/j.ceca.2009.03.011

Rohács, T., C.M. Lopes, I. Michailidis, and D.E. Logothetis. 2005. $PI(4,5)P_2$ regulates the activation and desensitization of TRPM8 channels through the TRP domain. *Nat. Neurosci.* 8:626–634. doi:10.1038/nn1451

Rosenhouse-Dantsker, A., and D.E. Logothetis. 2007. Molecular characteristics of phosphoinositide binding. *Pflugers Arch.* 455:45–53. doi:10.1007/s00424-007-0291-6

Runnels, L.W., L. Yue, and D.E. Clapham. 2002. The TRPM7 channel is inactivated by $PIP_{(2)}$ hydrolysis. *Nat. Cell Biol.* 4:329–336.

Smith, G.D., M.J. Gunthorpe, R.E. Kelsell, P.D. Hayes, P. Reilly, P. Facer, J.E. Wright, J.C. Jerman, J.P. Walhin, L. Ooi, et al. 2002. TRPV3 is a temperature-sensitive vanilloid receptor-like protein. *Nature.* 418:186–190. doi:10.1038/nature00894

Ständer, S., C. Moormann, M. Schumacher, J. Buddenkotte, M. Artuc, V. Shpacovitch, T. Brzoska, U. Lippert, B.M. Henz, T.A. Luger, et al. 2004. Expression of vanilloid receptor subtype 1 in cutaneous sensory nerve fibers, mast cells, and epithelial cells of appendage structures. *Exp. Dermatol.* 13:129–139. doi:10.1111/j.0906-6705.2004.0178.x

Stein, A.T., C.A. Ufret-Vincenty, L. Hua, L.F. Santana, and S.E. Gordon. 2006. Phosphoinositide 3-kinase binds to TRPV1 and mediates NGF-stimulated TRPV1 trafficking to the plasma membrane. *J. Gen. Physiol.* 128:509–522. doi:10.1085/jgp.200609576

Sugimoto, T., C. Xiao, and H. Ichikawa. 1998. Neonatal primary neuronal death induced by capsaicin and axotomy involves an apoptotic mechanism. *Brain Res.* 807:147–154. doi:10.1016/S0006-8993(98)00788-4

Suh, B.C., and B. Hille. 2007. Regulation of KCNQ channels by manipulation of phosphoinositides. *J. Physiol.* 582:911–916. doi:10.1113/jphysiol.2007.132647

Suh, B.C., and B. Hille. 2008. PIP2 is a necessary cofactor for ion channel function: how and why? *Annu Rev Biophys.* 37:175–195. doi:10.1146/annurev.biophys.37.032807.125859

Sui, J.L., J. Petit-Jacques, and D.E. Logothetis. 1998. Activation of the atrial KACh channel by the betagamma subunits of G proteins or intracellular Na^+ ions depends on the presence of phosphatidylinositol phosphates. *Proc. Natl. Acad. Sci. USA.* 95:1307–1312. doi:10.1073/pnas.95.3.1307

Ufret-Vincenty, C.A., R.M. Klein, L. Hua, J. Angueyra, and S.E. Gordon. 2011. Localization of the PIP2 sensor of TRPV1 ion channels. *J. Biol. Chem.* In press.

Várnai, P., and T. Balla. 1998. Visualization of phosphoinositides that bind pleckstrin homology domains: calcium- and agonist-induced dynamic changes and relationship to myo-[^{3}H]inositol-labeled phosphoinositide pools. *J. Cell Biol.* 143:501–510. doi:10.1083/jcb.143.2.501

Voets, T., J. Prenen, J. Vriens, H. Watanabe, A. Janssens, U. Wissenbach, M. Bödding, G. Droogmans, and B. Nilius. 2002. Molecular determinants of permeation through the cation channel TRPV4. *J. Biol. Chem.* 277:33704–33710. doi:10.1074/jbc.M204828200

Voets, T., G. Owsianik, A. Janssens, K. Talavera, and B. Nilius. 2007. TRPM8 voltage sensor mutants reveal a mechanism for integrating thermal and chemical stimuli. *Nat. Chem. Biol.* 3:174–182. doi:10.1038/nchembio862

Wiedemann, C., T. Schäfer, and M.M. Burger. 1996. Chromaffin granule-associated phosphatidylinositol 4-kinase activity is required for stimulated secretion. *EMBO J.* 15:2094–2101.

Xiao, R., J. Tang, C. Wang, C.K. Colton, J. Tian, and M.X. Zhu. 2008a. Calcium plays a central role in the sensitization of TRPV3 channel to repetitive stimulations. *J. Biol. Chem.* 283:6162–6174. doi:10.1074/jbc.M706535200

Xiao, R., J. Tian, J. Tang, and M.X. Zhu. 2008b. The TRPV3 mutation associated with the hairless phenotype in rodents is constitutively active. *Cell Calcium.* 43:334–343. doi:10.1016/j.ceca.2007.06.004

Xu, H., I.S. Ramsey, S.A. Kotecha, M.M. Moran, J.A. Chong, D. Lawson, P. Ge, J. Lilly, I. Silos-Santiago, Y. Xie, et al. 2002. TRPV3 is a calcium-permeable temperature-sensitive cation channel. *Nature.* 418:181–186. doi:10.1038/nature00882

Xu, H., N.T. Blair, and D.E. Clapham. 2005. Camphor activates and strongly desensitizes the transient receptor potential vanilloid subtype 1 channel in a vanilloid-independent mechanism. *J. Neurosci.* 25:8924–8937. doi:10.1523/JNEUROSCI.2574-05.2005

Xu, H., M. Delling, J.C. Jun, and D.E. Clapham. 2006. Oregano, thyme and clove-derived flavors and skin sensitizers activate specific TRP channels. *Nat. Neurosci.* 9:628–635. doi:10.1038/nn1692

Yoshioka, T., K. Imura, M. Asakawa, M. Suzuki, I. Oshima, T. Hirasawa, T. Sakata, T. Horikawa, and A. Arimura. 2009. Impact of the Gly573Ser substitution in TRPV3 on the development of allergic and pruritic dermatitis in mice. *J. Invest. Dermatol.* 129:714–722. doi:10.1038/jid.2008.245

Zhang, H., L.C. Craciun, T. Mirshahi, T. Rohács, C.M. Lopes, T. Jin, and D.E. Logothetis. 2003. $PIP_{(2)}$ activates KCNQ channels, and its hydrolysis underlies receptor-mediated inhibition of M currents. *Neuron.* 37:963–975. doi:10.1016/S0896-6273(03)00125-9

Zhang, Z., H. Okawa, Y. Wang, and E.R. Liman. 2005. Phosphatidylinositol 4,5-bisphosphate rescues TRPM4 channels from desensitization. *J. Biol. Chem.* 280:39185–39192. doi:10.1074/jbc.M506965200

Zhu, Y., X.R. Wang, C. Peng, J.G. Xu, Y.X. Liu, L. Wu, Q.G. Zhu, J.Y. Liu, F.Q. Li, Y.H. Pan, et al. 2009. Induction of leukotriene $B_{(4)}$ and prostaglandin $E_{(2)}$ release from keratinocytes by protease-activated receptor-2-activating peptide in ICR mice. *Int. Immunopharmacol.* 9:1332–1336. doi:10.1016/j.intimp.2009.08.006

Zufall, F., H. Hatt, and S. Firestein. 1993. Rapid application and removal of second messengers to cyclic nucleotide-gated channels from olfactory epithelium. *Proc. Natl. Acad. Sci. USA.* 90:9335–9339. doi:10.1073/pnas.90.20.9335